Hydrogel-Based Dye-sensitized Solar Cells

by

Hussain Jamali

A thesis

presented to the University of Waterloo

in fulfillment of the

thesis requirement for the degree of

Master of Applied Science

in

Electrical and Computer Engineering

Waterloo, Ontario, Canada, 2024

© Hussain Jamali 2024

Author’s Declaration

I hereby declare that I am the sole author of this thesis. This is a true copy of the thesis, including any required final revisions, as accepted by my examiners.

I understand that my thesis may be made electronically available to the public.

Abstract

This thesis delves into the exploration of Polyacrylamide (PAAm) hydrogel-based solar cells, scrutinizing their design, performance, and inherent challenges. The three-layered PAAm solar cell, featuring high-salinity (HS) and low-salinity (LS) layers, exhibited promising outcomes, with FTO and Aluminum identified as optimal back electrodes. However, critical limitations were uncovered, including sensitivity to thickness variations and the adverse effects of extended curing times on ion diffusion. In response, a proposed shift to a simplified two-layered structure presented comparable performance, addressing these challenges. Furthermore, recognizing the limitations of PAAm design, this research introduces the prospect of a Polyvinyl Alcohol-Polyaniline (PVA-PANI) Dye-Sensitized Solar Cell (DSSC). The proposed PVA-PANI DSSC aims to overcome regeneration constraints and broaden photon absorption, leveraging PVA-PANI's distinctive properties for enhanced efficiency. Additionally, the study aims to understand the relationship between hydrogel composition, structure, and solar cell performance, to optimize the formulation for enhanced stability and overall device efficiency.

The study focuses on creating and evaluating a unique hydrogel formulation made of PVA-PANI that is impregnated with an iodide/triiodide electrolyte to simulate DSSC operation. The goal is to compare the impact of these hydrogel-based quasi-solid-state electrolytes on device efficiency and stability through a systematic analysis. The research also explores the impact of the degree of cross-linking within the hydrogel structures, and how it affects electrical conductivity, ion diffusion, and mechanical integrity.

This investigation contributes valuable insights to the evolving landscape of hydrogel-based solar cells, bridging the gap between theoretical potential and practical implementation in sustainable energy solutions. The research findings are expected to have practical applications in sustainable energy systems, thus helping us move closer towards a greener and more sustainable future.

Acknowledgements

I am extremely grateful to Professor Sheva Naahidi for her constant support, encouragement and invaluable guidance throughout my tenure as her student. I am deeply thankful to her for giving me the opportunity to be a part of her research group.

In addition, I extend my heartfelt appreciation to Professor Majedi for allowing me access to his laboratory and for the insightful discussions that proved to be instrumental in my research.

I would also like to express my gratitude to my entire family for their unwavering support and encouragement throughout this journey.

Finally, I would like to acknowledge the collective efforts of everyone who contributed to the completion of this thesis. Your contributions are greatly appreciated.

Dedication

To my father and grandfather.

Table of Contents

Author's Declaration ..... *ii*

Abstract ..... *iii*

Acknowledgements ..... *iv*

Dedication ..... *v*

List of Figures ..... *viii*

List of Tables ..... *ix*

Chapter 1: Introduction *1*

1.1 Motivation & Background **1**

1.3 Research Objectives **4**

Chapter 2: Literature Review *6*

2.1 Bio-inspired Solar Cells **6**

2.2 Ionotronic Devices **8**

2.3 Hydrogels **9**

i. Composition of Hydrogels 10

ii. Types of Hydrogels 12

iii. Swelling of Hydrogels 14

iv. Poly Vinyl-Alcohol (PVA) Hydrogels 15

v. Poly Acrylamide (PAAm) Hydrogels 15

2.4 Hydrogels in Ionotronic Devices **16**

2.5 Polyacrylamide Hydrogel-Based Solar Cell **18**

i. Working Principles 25

ii. Limitations 27

2.6 Dye-Sensitized Solar Cell (DSSC) **29**

i. Photoanode 31

ii. Electrolyte 37

iii. Counter electrode (CE) 40

2.7 Evaluation of DSSC Performance **42**

i. Model of a Solar Cell 44

Chapter 3: Methodology 49

3.1 Materials 49

3.2 Synthesis of Polyacrylamide (PAAm) Solar Cell 49

3.3 Fabrication of DSSC 49

i. Photoanode 49

ii. Hydrogel Electrolyte 50

iii. Assembling DSSC 52

3.4 Measurements 52

i. Photovoltaic Measurements 52

ii. Swelling Measurements of Hydrogel 52

iii. Mechanical Measurement of Hydrogel 53

Chapter 4: Results & Discussion 54

4.1 Effect of Preparation Method on PVA-Hydrogel 54

i. Effect of Physical Parameters 54

ii. Effect of PVA Concentrations 56

iii. Effect of Crosslinking 58

4.2 Photovoltaic Performance of Hydrogel-Based Solar Cells 59

i. Polyacrylamide (PAAm) Hydrogel-Based Solar Cell 60

ii. PVA-PANI Hydrogel-Based DSSC 66

Chapter 5: Conclusion 72

5.1 Future Prospects 74

References 77

List of Figures

Figure 1 [19] Shalini, S., et al. "Status and outlook of sensitizers/dyes used in dye sensitized solar cells (DSSC): a review." International journal of energy research 40.10 (2016): 1303-1320. 31
Figure 2 Ionotronic Solar Cell Structure 32
Figure 3 Ionotronic Solar Cell at Equilibrium 33
Figure 4 Neutralization of Ionotronic Solar Cell. 34
Figure 5: a) Picture of Ionotronic Solar Cell. b) Illuminated I-V for Ionotronic Solar Cell. c) UV-Vis Spectra of Ionotronic Solar Cell 35
Figure 6 Proposed Structure 36
Figure 7 [35] Wang, Kai, et al. "Chemically crosslinked hydrogel film leads to integrated flexible supercapacitors with superior performance." Advanced materials 27.45 (2015): 7451-7457 54
Figure 8: a) Hydrogel obtained at 90°C reaction temperature. b) Hydrogel annealed after reaction at room temperature. 56
Figure 9: a) 5 wt% PVA-PANI Hydrogel. b) 7.5 wt% PVA-PANI Hydrogel. c) 10 wt% PVA-PANI Hydrogel. d) 12.5 wt% PVA-PANI Hydrogel. 57
Figure 10 Stretchability of 10 wt% PVA 58
Figure 11: a) 2.5 wt% PANI hydrogel. b) 5 wt% PANI hydrogel. 67
Figure 12 Dark IV of DSSC with different concentrations of PANI 68
Figure 13 Illuminated IV for hydrogel based DSSC. 70
Figure 14 Proof of Concept 71
Figure 15 Proposed Working Electrode 74
Figure 16 Proposed hydrogel-based electrolyte 75
Figure 17 Proposed Counter Electrode 75
Figure 18 Proposed DSSC 76

List of Tables

Table 1 [4] L.-Y. Lin and K.-C. Ho, “Dye-sensitized solar cells,” Encyclopedia of Modern Optics, pp. 270–281, 201 37
Table 2 Swelling ratio for different crosslinking ratios 59
Table 3 Isc & Voc for different electrolytes 69

Chapter 1: Introduction

Renewable energy is a constantly evolving field, and introducing new materials is crucial to improving solar cell technology. This thesis focuses on the use of bio-inspired hydrogels in solar cells, with the goal of enhancing their efficiency and addressing current challenges. Our research team is at the forefront of this innovation, exploring the intersection of hydrogel science and photovoltaics to make significant contributions to the development of sustainable solar cell technology.

1.1 Motivation & Background

The use of traditional solar cells has been limited by factors such as instability, environmental impact, and low efficiency. Solar cell production processes typically involve energy-intensive steps, from raw material extraction to semiconductor manufacturing. This results in a significant carbon footprint and resource consumption. However, hydrogel-based solar cells offer a sustainable alternative. Hydrogels are synthesized from water-based solutions and polymers, making them eco-friendly and energy-efficient. The malleability and water-based nature of hydrogels contribute to reduced energy consumption during the manufacturing process, as they can be molded and structured with ease. The efficiency of hydrogel-based solar cell fabrication aligns with environmental sustainability goals and highlights the potential for a more energy-efficient future in solar cell technology.

To overcome these limitations, our research group has been working on exploring and utilizing the unique properties of hydrogels. These water-absorbent materials have excellent water-retention capabilities and biocompatibility, making them a promising solution for overcoming the challenges associated with solar energy adoption. Our former researchers conducted pioneering work within our research group, exploring innovative approaches to enhancing solar cell performance. This research involved the development

of ionotronic energy pathways that were inspired by the electric eel. By drawing inspiration from nature, the work highlighted the potential of incorporating hydrogels in solar cells to optimize energy pathways. This exploration aligns with our research group's commitment to advancing sustainable and efficient solar cell technologies through novel materials and design principles.

Their work introduced a fascinating concept by utilizing ion transport mechanisms to generate energy within hydrogels, which could potentially replace conventional solar cells. However, every groundbreaking research has its limitations and offers opportunities for further exploration. My thesis aims to build upon the innovative idea and overcome some of the drawbacks in their initial study.

The proposed design for developing solar cells initially suggested using a 3-layered Polyacrylamide (PAAm) hydrogel structure with high-salinity (HS) - low-salinity (LS) - high-salinity (HS) salt concentration gradients. The incorporation of salt concentration gradients showcased the potential for creating a self-sustaining energy source. However, upon further examination, a 2-layered structure consisting of HS-LS provided similar results. This two-layered structure generated a high open-circuit voltage of approximately 4.5V when exposed to light. One of the primary challenges with this design was the inability to regenerate the potential gradient within the device after it had been used. This limitation could have significant implications for the efficiency and practicality of the technology, as it could impact its long-term operation and energy output. Additionally, the use of hydrogels as a light absorber limited the device's ability to absorb photons in the visible range, which required the addition of photoactive compounds to enhance absorption.

To address the limitations of the previous design, my thesis proposal suggests a transformative solution. I propose the development of a Dye-Sensitized Solar Cell (DSSC) configuration, which will use a hydrogel as a quasi-solid-state electrolyte. By doing so, I aim to overcome the challenges in the original design by incorporating a counter electrode and adding a photoactive compound to the other electrode to regenerate the potential

gradient and also increase the absorption spectrum of the device. In a DSSC, the quasi-solid-state electrolyte allows for more efficient ion transport and energy regeneration, addressing the critical issue of potential gradient depletion. By leveraging the unique properties of hydrogels as a versatile and water-based medium, we can explore the incorporation of photoactive compounds for superior absorption in the visible range. This approach has the potential to revolutionize the device's performance in harnessing solar energy, making it more adaptable to a wider range of environmental conditions and light sources.

Hydrogels are unique polymeric materials that have the ability to swell in liquid without dissolving. What makes hydrogels even more special is their 3D network structures, which give them an increased capacity to hold liquid, unlike other polymers. This allows ions in the liquid electrolyte to move more freely within the hydrogel, resulting in high energy conversion efficiency and a more effective quasi-solid gel medium. On a molecular level, the polar solvent in hydrogels can either bond to polar hydrophilic groups through Van der Waals attraction and hydrogen bonding, or fill the space between the network chains, pores, or voids. The changeable composition, adaptable structure, manageable electronic capabilities, and effective adsorption traits have elevated hydrogel's status as a promising contender for constructing 3D frameworks.

In addition, the semiconductor layers used in DSSCs are usually anchored onto a variety of substrates through simple physical adsorption. However, they still exist on the substrate as two-dimensional (2D) materials. Consequently, this leads to the reduction of the overall photocurrent efficiency as only the surface of the material can effectively utilize the light energy. By incorporating phosphorescence or luminous chromophores, such as by adding energy relay dyes (ERDs) to the quasi-solid-state electrolyte and rare-earth doped oxides to the DSSC, one can improve the photocurrent efficiency. Hydrogels with good light transmittance and refractive properties enable uniform light distribution to the ERDs inside the hydrogel, effectively harnessing light energy to enhance photocurrent. Hydrogels have a three-dimensional porous structure and suitable nanopore size distribution, providing a large number of reaction sites for the ERDs.

In conclusion, my thesis represents a pivotal advancement in the field of ionotronic solar cells by addressing the shortcomings identified in the original work. By transitioning to a DSSC with a hydrogel-based quasi-solid-state electrolyte, we stand to make significant strides in achieving the efficiency and practicality required for the widespread adoption of this promising technology. This thesis underscores our commitment to advancing renewable energy solutions and contributing to a more sustainable future.

1.3 Research Objectives

The research objectives of this thesis revolve around exploring the utilization of hydrogels as quasi-solid-state electrolytes in DSSCs. The primary aim is to investigate the feasibility of hydrogels as an alternative electrolyte medium to address the stability and efficiency challenges often associated with traditional liquid electrolytes in DSSCs. This study seeks to comprehensively evaluate the electrical conductivity, charge transport capabilities, and photovoltaic performance of hydrogel-based quasi-solid-state electrolytes. Additionally, the research endeavours to elucidate the interplay between hydrogel composition, structure, and DSSC performance, aiming to optimize the formulation for enhanced stability and overall device efficiency. Two types of hydrogel solar cells were studied: a two-layered polyacrylamide hydrogel solar cell that utilizes a salt concentration gradient, and a PVA-PANI hydrogel-based DSSC.

A study was conducted to explore the properties of a two-layered polyacrylamide hydrogel-based solar cell, with the aim of improving its photovoltaic performance. The study looked at various factors that could enhance the efficiency and power output of the solar cell under different conditions. In particular, the impact of salinity gradients was investigated by implementing high-salinity and low-salinity layers, and the use of different salts sodium chloride (NaCl) and potassium chloride (KCl) was analyzed. The effects of different electrode materials aluminum (Al), copper (Cu), and fluorine-doped tin oxide (FTO) on performance were also studied. Finally, the study looked at optimizing the thickness of the layers to maximize light absorption and electron transport.

This study also encompasses the development and assessment of PVA-PANI hydrogel a distinct hydrogel formulation. The hydrogel is subsequently impregnated with an iodide/triiodide electrolyte, simulating the operational conditions of DSSCs. By systematically comparing the performance of these hydrogel-based quasi-solid-state electrolytes, their respective impact on the overall device efficiency and stability is thoroughly examined. Furthermore, the investigation extends to the influence of the degree of cross-linking within the hydrogel structures. The effect of varying degrees of cross-linking on the electrical conductivity, ion diffusion, and mechanical integrity of the hydrogel electrolytes will be scrutinized.

Through these multifaceted analyses, this research endeavours to not only shed light on the potential of hydrogel-based electrolytes in DSSCs but also to provide insights into the nuanced relationship between hydrogel composition, cross-linking density, and their performance attributes. Additionally, the research will assess the long-term stability and durability of the hydrogel-based solar cell under operational conditions. This holistic approach to understanding hydrogel-based quasi-solid-state electrolytes in DSSCs is expected to contribute significantly to the advancement of next-generation solar energy conversion technologies. By achieving a thorough understanding of the electrochemical and optoelectronic properties of hydrogel-based electrolytes within the context of DSSCs, this research aspires to contribute to the advancement of more reliable and efficient solar energy conversion technologies with potential applications in sustainable energy systems.

Chapter 2: Literature Review

The literature review chapter delves into a comprehensive exploration of the existing body of knowledge surrounding the utilization of hydrogels in ionotronic devices. This chapter critically examines research efforts, experimental methodologies, and findings that have contributed to our understanding of hydrogel-based electrolyte systems within the context of solar energy conversion. By synthesizing information from a diverse range of sources, this chapter aims to establish a foundation for the current state of the field. Through an in-depth analysis of the evolution of DSSCs, the review identifies key challenges, trends, and advancements, thereby paving the way for the understanding of the research landscape and setting the stage for the original contributions of this study.

2.1 Bio-inspired Solar Cells

Nature has always been a source of inspiration for technological advancements, and solar cell design is no exception. By studying the complex mechanisms found in natural systems, we can gain valuable insights to improve the performance of solar cells. Biomimicry, which involves drawing inspiration from nature's designs and processes, offers a unique and innovative approach. For example, examining the efficiency of photosynthesis in plants has led to the exploration of organic materials that can imitate the light-harvesting capabilities of chlorophyll [1]. This exploration has notably led to the development of DSSC. DSSCs, pioneered by O'Regan and Grätzel in 1991, leverage the principles of light absorption observed in plant photosynthesis, using organic dyes to capture sunlight and convert it into electrical energy [2]. Moreover, bio-inspired designs, such as those influenced by the electric eel's ionotronic energy pathways, demonstrate how natural systems can help develop new energy conversion strategies [3]. By leveraging the inherent efficiency and adaptability of biological systems, we can create more sustainable, durable, and efficient solar cells, leading to the development of resilient and eco-friendly photovoltaic technologies.

The first and most important step in creating a solar device is to absorb light. To increase the efficiency of solar cells, it is crucial to maximize the collection of all types of light. There are three key principles that can help achieve this goal: light coupling at the initial contact surface, light trapping in weakly absorbed wavelength regions, and reducing optical losses. By addressing these principles, we can improve light harvesting and optimize the overall energy conversion efficiency.

Many insects showcase intricate surface structures designed to minimize light reflection, a feature that contributes to their adaptability in diverse environments. Smaller variations in refractive index can lead to reduced reflection, according to Fresnel's law. To create anti-reflective (AR) surfaces, researchers often take inspiration from the moth-eye structure. This unique structure consists of hexagonal arrays of cone-shaped protrusions (as shown in Figure 1), which introduce a gradual change in refractive index, thus reducing reflection. Kang, Seong Min, et al. [4], managed to increase the power conversion efficiency of perovskite solar cells by around 11% by incorporating a moth-eye pattern in the TiO_2 layer. This improvement is mainly due to the enhanced light harvesting efficiency achieved through the biomimetic design principles used in the moth-eye pattern, demonstrating the pattern's effectiveness in optimizing light absorption and improving the overall performance of perovskite solar cells.

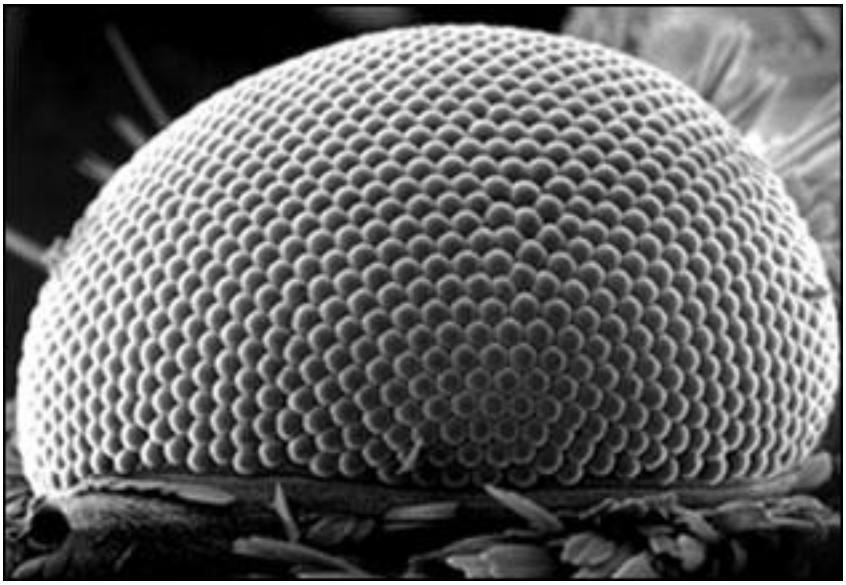


Figure 1 Scanning electron microscope image of the eye on a leaf miner moth. (Image: Dartmouth College)

Similarly, plants have evolved to absorb light efficiently for the conversion of solar energy into usable forms. Notably, some plant species have fine-tuned their light absorption processes to suit specific environmental conditions. Photosynthesis is known for its electron transport mechanisms. The electron transport chain is a complex system of proteins that generates and separates charges. This process is fueled by solar energy and facilitated by redox reactions in photosystems 1 and 2. The low recombination rate of these photosystems ensures efficient charge separation, which results in the generation of sustenance for photosynthetic organisms. In modern bioinspired photovoltaic research, emulating natural photosynthesis is an important goal for achieving efficient energy conversion in artificial systems.

One promising approach is to draw inspiration from nature and mimic the structures that have evolved to be highly efficient in light absorption. This biomimicry can help improve the light-capturing capabilities of solar cell technologies, leading to significant advancements in energy conversion efficiency.

2.2 Ionotronic Devices

Ionotronic devices are a new class of electronic systems that use the controlled movement of ions rather than traditional electronic charges to manipulate and adjust electronic properties. Although ions generally have lower mobility compared to electrons, this perceived disadvantage is offset by significant advantages in other important areas. The potential of ionotronic devices to revolutionize electronic systems by introducing new levels of adaptability, flexibility and responsiveness opens up exciting possibilities for the development of next-generation electronics. In ionotronics, ions such as anions or cations work as active carriers alongside electrons, allowing for dynamic modulation of electronic conductance. This innovative approach has shown promise in various applications, ranging from bioelectronic interfaces to energy storage devices. The growing field of ionotronics harnesses the synergistic interplay between ionic and electronic components, providing a new way to design advanced devices with unique functionalities.

Ionotronic devices have a significant advantage in energy storage technologies, where they utilize ion transport to store and release charges efficiently. The collaboration between ionic and electronic components creates new opportunities for developing high-performance batteries and capacitors. Additionally, the combination of ions and electrons in ionotronics has enormous potential to revolutionize the fields of sensing and computation. As research in ionotronics continues to advance, the industry is positioned to provide transformative solutions that leverage the unique advantages of ions. This technology can bridge the world of slow ion mobility to the exciting possibilities of innovation in electronics, energy storage, and interdisciplinary research.

Hydrogels are very promising materials in the field of ionotronics. They have unique properties that allow them to absorb liquids within their network, making them ideal for ionotronic devices. Hydrogels are water-absorbent polymer networks that have high water content and are compatible with ionic solutions. This makes them perfect for ionotronic devices, as they allow for the incorporation of ions within the hydrogel structure to facilitate controlled ionic movement. Combining hydrogels with ionotronic principles opens up new possibilities for creating responsive and adaptable devices. Hydrogel-based ionotronic systems have already been used in energy storage devices, wearable devices, and biomedical sensors. The synergistic interplay between ions and hydrogel properties allows for precise control and modulation of electronic functionality.

2.3 Hydrogels

Hydrogels are unique structures made of a three-dimensional crosslinked polymer meshwork, which have the ability to absorb large amounts of water or other liquids and maintain their structure even when swollen. This is made possible by the presence of polar hydrophilic moieties, such as SO_3H, OH, NH_2, $COOH$, $CONH_2$, which are attached to the polymer network as branched groups. The hydrophilicity of these groups, along with the strength of the crosslinking, determines the degree of water absorption while maintaining the network structure. Hydrogels have unique properties such as biodegradability, biocompatibility, hydrophilicity, super absorbency, viscoelasticity, softness, and fluffiness, making them ideal for a variety of applications. Additionally,

hydrogels can respond to various stimuli, including temperature, electric field, magnetic field, biological molecules, and ionic strength.

In recent times, hydrogels have caught the attention of researchers for their potential in energy storage and conversion applications. This is because they possess a semi-solid form and are naturally flexible. Traditional energy storage and conversion devices are typically heavy, mechanically rigid, and unsustainable. Moreover, commercially available devices often contain liquid electrolytes, which can cause device leakage and are harmful to humans due to their organic nature. To address these issues, hydrogel electrolytes have been introduced into these devices. These electrolytes are semi-solid, biocompatible, biodegradable, cost-effective, and environmentally friendly. Devices that utilize hydrogels for energy storage and conversion become flexible, stretchable, and elastic, and can work under stretching, bending, folding, and twisting. These characteristics are a significant improvement over traditional electrochemical devices. Furthermore, hydrogels possess self-healing properties, which is a critical element for wearable and portable electronic devices. The ability to self-heal or manage damage makes these devices ideal for smart and lightweight electronics.

Hydrogels are classified based on the polymers used, their source, crosslinking method, stimuli response, and ionic charge. Polymers can be natural, synthetic, or a combination. Hydrogels are made by crosslinking polymers, which can be achieved through physical, chemical, or both methods simultaneously. Crosslinked polymers are known as hydrogels whether they are made from synthetic polymer or natural polymer. There are different ways to crosslink, like mixing, solution casting, bulk polymerization, free radical polymerization, UV and gamma irradiation, and interpenetrating network formation. Hydrogels can be categorized based on their ionic charge as cationic, anionic, or neutral. The charge of the whole network is determined by the charge on the polymer.

i. Composition of Hydrogels

Hydrogels made from natural polymers are called natural polymer hydrogels. These polymers can be sourced from various natural sources and are divided into three

categories - neutral, cationic, and anionic. Natural polymers are easy to obtain, abundant, cheap, non-toxic, and biodegradable, and possess many other beneficial biological properties. However, hydrogels produced from natural polymers such as chitosan and other polysaccharides are delicate. Natural polymers are crosslinked, grafted with monomers, or blended with synthetic polymers to enhance their mechanical properties. For instance, synthetic polymer polyvinyl alcohol (PVA) is used as a blending agent to boost natural polymers' mechanical strength and elasticity [5].

Hydrogels made from synthetic polymers offer greater flexibility in adjusting their mechanical properties. These polymers are preferred over natural polymers as they offer better control over physical and chemical properties. Synthetic polymers can be produced with long-chain structures and high molecular weight, making them ideal for hydrogel synthesis. Some examples of synthetic polymers used in hydrogel synthesis are polyvinyl alcohol (PVA), polyethylene glycol (PEG), poly (ethylene oxide) (PEO), poly (2-hydroxyethyl methacrylate) (PHEMA), poly (acrylic acid) (PAA), and poly (acrylamide) (PAAm), etc. Owing to its excellent physical properties, such as excellent chemical resistance, biodegradability, and biocompatibility, polyvinyl alcohol (PVA) has attracted increasing attention.

Conductive hydrogels possess the ability to conduct electricity due to the inclusion of conductive materials in their composition, such as carbon nanotubes [6] and graphite [7]. Graphene has also been introduced in hydrogels because of its exceptional Young's modulus (1 TPa), electrical conductivity (6000 S cm^{-1}), and high surface area (2630 m^2 g^{-1}) [8]. However, adding these materials directly can decrease hydrogels' transmission capacity significantly. As a solution, conductive polymers like polyaniline (PANI) [9], polypyrrole (PPy) [10], and polythiophene (PTh) [11] are added to improve conductivity while maintaining soft mechanical properties. These organic semiconductors provide electronic conductivity and contribute ions in aqueous media, making them more advantageous than traditional conductive materials. Furthermore, many polymers can form hydrogels and carry various functional groups.

ii. Types of Hydrogels

Hydrogels are classified into three types based on the crosslinking forces between their polymeric chains: chemical hydrogels, physical hydrogels, and hybrid hydrogels which combine both types of crosslinking. Physical hydrogels are formed due to non-covalent forces between polymer chains, such as hydrogen bonding, ionic forces, Van der Waals interactions, polyelectrolyte complexation, stereocomplexation, and hydrophobic forces. They are disordered, fragile, and weak when exposed to external stimuli as the interactions between polymer chains are not very strong. Physical hydrogels show a reversible response to environmental changes and usually dissolve in organic solvents and water upon heating. In contrast, chemical hydrogels involve covalent bonding between polymer chains and do not dissolve in the surrounding medium. They are known as permanent hydrogels as they do not show a reversible response as physical hydrogels do. Chemical crosslinking occurs through various means, utilizing small molecules such as formaldehyde, glutaraldehyde (GA), genipin, diglycidyl ether, and N, N'-methylenebisacrylamide. The crosslinkers form covalent bonds with the polymers through condensation reaction or free radical mechanism. For condensation reactions, the crosslinker should contain two functional groups typically (GA) [12] while a mono-functional group containing a crosslinker like formaldehyde [13] can also be used. In the free radical mechanism, the crosslinker must contain at least two double bonds. Chemical crosslinking imparts excellent thermal, mechanical, chemical, and surface properties to the prepared hydrogels and maintains the network structure of hydrogels in a fully swollen state.

For a polymer network to form a hydrogel, it needs to have strong inter-chain interactions to create a stable molecular network, as well as encourage water access and retention. Physical hydrogels can be produced through non-covalent approaches, such as electrostatic, hydrogen bonding, and hydrophobic forces among polymer chains. These interactions create physical gels that have high water sensitivity and thermo-reversibility. Non-ionic polymers can also form physical hydrogels through freeze-drying or freeze-thawing cycles, where they create intersection points in the form of crystallites. Crystallization due to the association of chains via hydrogen bonding is most likely the

cause behind the development. To illustrate, a PVA solution in water forms a gel with low mechanical strength when left at room temperature. However, after undergoing freeze-thaw cycles, the solution turns into a PVA hydrogel. The mechanical strength of the hydrogel increases significantly compared to its previous state before the freeze-thaw process. The strength and properties of hydrogels depend on several factors, including the concentration of PVA, and the number of freeze-thawing cycles [14]. The addition of polysaccharides such as chitosan, reduced the crystallinity of PVA hydrogels, dextran increased the process of crystallization of PVA hydrogels, and alginate increased the mechanical strength of the PVA hydrogels [15].

The formation of physical gels through the clustering of molecules causes the formation of free chain loops and thus inhomogeneity that signifies short-lived network imperfections. Hydrogels that are cross-linked chemically are formed by polymerizing monomers while using cross-linking agents like heat, light, radiation, and mechanical force. These agents work as bridging agents between linear molecules, allowing them to bond and cross-link to form network structures. This helps in the formation of covalent or ionic bonds between the polymeric molecular chains. Some of these cross-linking agents can be toxic, but physically cross-linked hydrogels can be gelatinized without the use of any toxic chemical cross-linking agent or catalyst.

A technique for preparing hydrogels using light-sensitive functional groups has significant advantages over chemical crosslinking methods. This technique is easy, fast, and cost-effective. Chemically crosslinked hydrogels can be developed by initiating reactions using an initiator such as potassium persulfate (KPS), ammonium persulfate (APS), ceric ammonium nitrate, ferrous ammonium sulfate, 2-20-azobisisobutyronitrile (AIBN), and benzoyl peroxide. Crosslinked polymer networks can also be reinforced by interlocking secondary polymers within the entangled networks. When the entangled polymer networks are allowed to swell in an aqueous solution in the presence of polymerizable monomers, they are called interpenetrating polymer networks (IPNs). An IPN is a polymer comprising two or more networks that are at least partially interlaced at a molecular scale but not covalently bonded to each other. If one polymer network is crosslinked while the

other polymer physically associates with the crosslinked polymer, the network formed is called a semi-interpenetrating polymer network (semi-IPN). If the second polymer undergoes crosslinking alongside the pre-existing crosslinked polymer network, the resulting structure is called a full-interpenetrating polymer network (full-IPN). Figure 2 shows the composition of a hydrogel with its parameters.

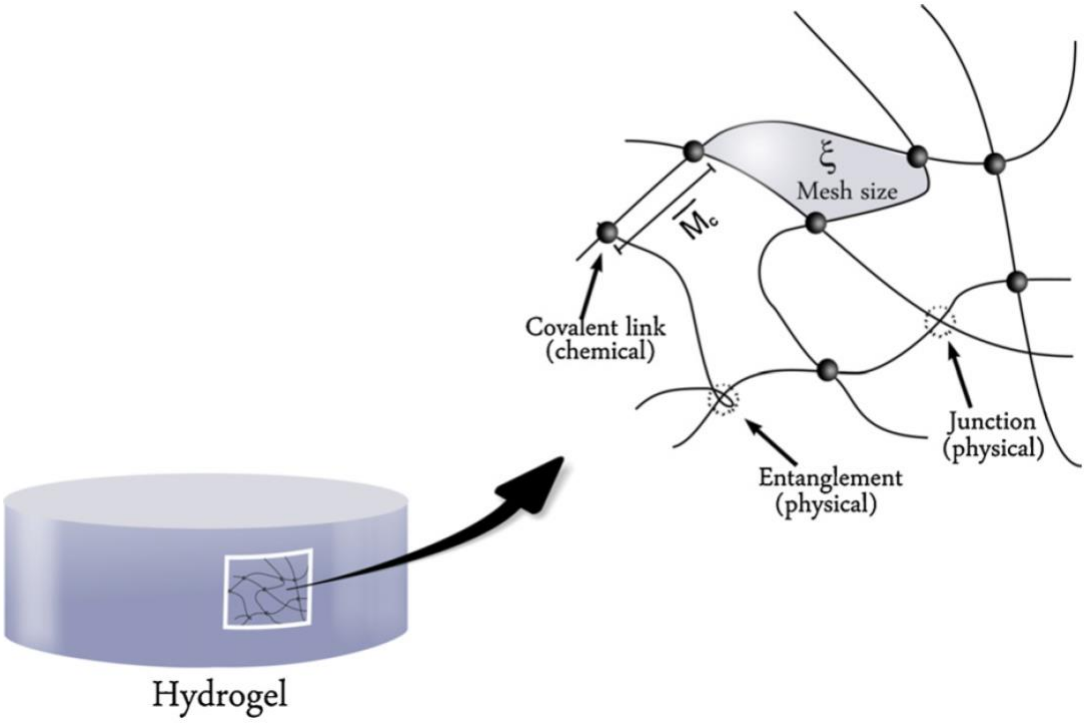


Figure 2 A cross-linked hydrogel structure with the mesh size ξ and the average molecular weight between the cross-linking points $\overline{M_C}$, respectively. ([16] Buenger, Daniel, Fuat Topuz, and Juergen Groll. "Hydrogels in sensing applications." Progress in Polymer Science 37.12 (2012): 1678-1719.)

iii. Swelling of Hydrogels

Hydrogels have the unique ability to swell, which is a crucial aspect of their existence. This swelling occurs in three steps: first, water diffuses into the hydrogel network, then the polymer chains relax, and finally, the hydrogel network expands. In its dehydrated state, a hydrogel is called the glassy state, while in its swollen form, it is referred to as the rubbery state. When the dry hydrogel comes into contact with an aqueous medium, the free spaces in the chains allow solvent molecules to occupy them. As more water enters the hydrogel matrix, the glassy state transforms into the rubbery state, which is known as

swelling. The diffusion process is responsible for the entry and exit of water from the hydrogel matrix. Swelling is measured by the swelling ratio, which is the weight swelling ratio of the swollen gel to the dry gel. According to the Flory-Reihner theory, the elastic nature of the polymer chains and their compatibility with water molecules determine the swelling of hydrogels [17]. The swelling ratio is affected by the amount of crosslinking, highly crosslinked structures have a lower swelling ratio. The swelling of hydrogels is also affected by the presence of hydrophilic and hydrophobic groups on the polymer chains. Temperature and pH also affect the swelling of hydrogels. pH-sensitive hydrogels swell due to the ionization of hydrophilic groups with variations in pH levels. Covalently crosslinked hydrogels that contain ionic pendant groups respond to changes in pH and are known as pH-responsive hydrogels. Hydrogels with anionic groups swell at a higher pH, while hydrogels containing cationic groups swell at a low pH.

iv. Poly Vinyl-Alcohol (PVA) Hydrogels

PVA, also known as polyvinyl alcohol, is a synthetic polymer that has been receiving increasing attention due to its outstanding physical properties such as biocompatibility, biodegradability, and chemical resistance [18]. Hydrogels that are formed with PVA have been found to be particularly effective. In a study conducted by Chen et al. [19], six different types of PVA-based hydrogels were examined for their supercapacitor performance. These hydrogels used different types of electrolytes, including H_sSO_4, KOH, NaOH, NaCl, H_3PO_4, and KCl. The results showed that the PVA-H_3PO_4 hydrogel electrolyte had the finest capacitive performance among all the PVA-based hydrogels. PVA-based hydrogel electrolytes are commonly used to make flexible supercapacitors because they are affordable, non-toxic, and chemically stable [20]. One way to improve the chemical and mechanical properties of original PVA-based hydrogel electrolytes is by crosslinking them with glutaraldehyde (GA) [21].

v. Poly Acrylamide (PAAm) Hydrogels

Many acrylamide hydrogels have been prepared and utilized in numerous fields. PAAm hydrogels are hydrophilic, neutral, and possess significant valuable physical and chemical properties for potential applications as a biomaterial, for the immobilization of cells and

biocatalysts, in drug delivery systems, for heavy metal ions absorption, and as bio-separators. PAAm hydrogels are weak in hydrolytic stability and mechanical strength. Efforts have been made to ameliorate their properties by co-polymerization with other monomers. PAAm hydrogels are easy to synthesize, highly stretchable and transparent.

Although commonly used, polyacrylamide networks are covalently linked and thus do not heal after rupture. To provide healing, polyvinyl alcohol (PVA) and polyacrylic acid/alginate (PAAc/alginate) hydrogels can be used [22]. Hydrogels are susceptible to dehydration in air. Dissociation of a hygroscopic salt in water results in the formation of hydrated ions, decreasing the vapour pressure. The salts further stabilize the water in the hydrogels. Salts include sodium chloride and lithium chloride, which have similar conductivities, but sodium chloride has better biocompatibility, while lithium chloride has better water retention.

2.4 Hydrogels in Ionotronic Devices

Optoelectronic devices require a balance between optical transparency and electrical conductivity in their materials. However, conventional transparent electrodes like indium tin oxide (ITO) and fluorine tin oxide (FTO) have limitations due to their rigidity, brittleness, and high cost. This restricts their use in mobile and wearable devices. To solve this issue, researchers are developing stretchable and transparent electronic conductors using soft matrices that contain conducting materials, such as patterned conducting polymers. However, these alternatives have challenges like low stretchability, reduced transparency, and degradation during cyclic loading.

On the other hand, hydrogels offer an effective solution by achieving high transparency and stretchability without compromising conductivity. Although hydrogels have a higher resistivity than ITO, a millimeter-thick hydrogel can achieve a surface resistance of 100 Ω sq−1 while maintaining an optical transparency of 99.9% [23]. The softness of hydrogels allows for extensive and elastic deformation over numerous cycles, maintaining conductivity even under high stretching. Moreover, hydrogel properties can be tailored by adjusting their components, enabling the creation of robust hydrogels resembling natural

rubber and those that retain water in low-humidity environments. These features make hydrogels ideal for electrodes in electro-optical devices, offering a blend of electro-optical performance and remarkable stretchability.

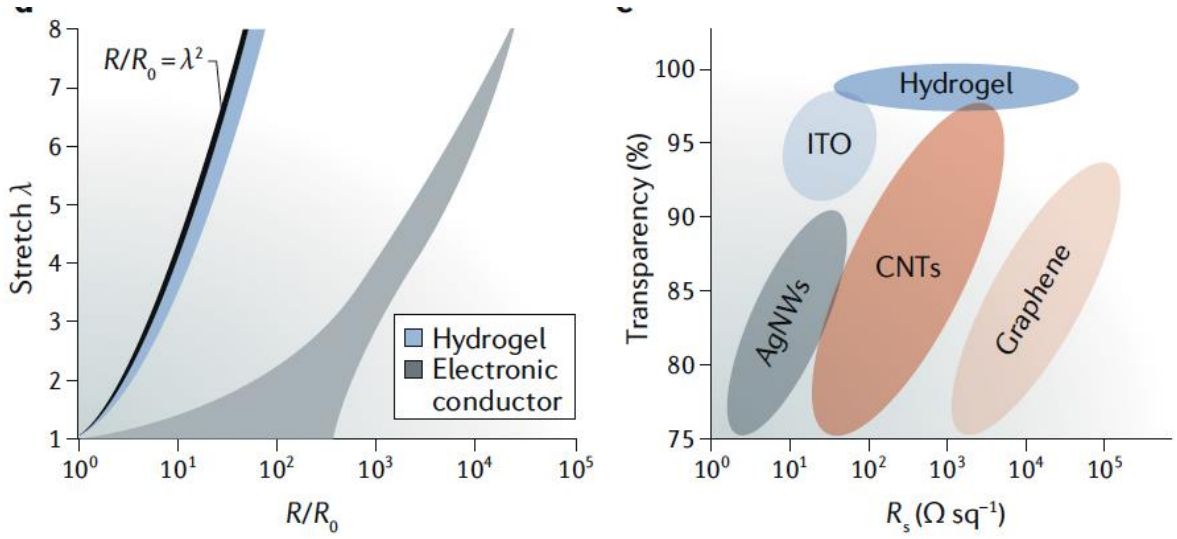


Figure 3 Hydrogels as stretchable electrodes ([23] Keplinger, Christoph, et al. "Stretchable, transparent, ionic conductors." Science 341.6149 (2013): 984-987)

In Figure 3, it is evident that electronic conductors break at a smaller stretch (λ) compared to hydrogels. At low resistance (Rs), electronic conductors are less transparent than hydrogels. The abbreviations used in the figure are as follows: AgNWs (silver nanowires), CNTs (carbon nanotubes), ITO (indium tin oxide), R (electrical resistance in the stretched state), and R0 (electrical resistance in the initial state).

Hydrogels with a three-dimensional structure can significantly enhance the performance of DSSC. The 3D structure of hydrogels offers a unique advantage over traditional flat configurations, as it provides an increased surface area for light absorption and dye loading. This expanded surface area allows for more efficient utilization of incident light, leading to enhanced photon capture and improved energy conversion efficiency. Furthermore, the porous nature of 3D hydrogel structures facilitates better electrolyte penetration, promoting effective charge transport within the solar cell. By incorporating phosphorescence or luminous chromophores, such as by adding ERDs to the quasi-solid-

state electrolyte and rare-earth doped oxides to the DSSC, one can improve the photocurrent efficiency.

The electroluminescent device, introduced in the research papers by Yang, Can Hui et al. [24] and Larson, Christina et al. [25], represents a major breakthrough in the field of stretchable electronics. By seamlessly integrating electronic and ionic components, this innovative device achieves remarkable stretchability. It relies on phosphor powders as electroluminescent materials, which enhances its emissive properties. Additionally, the device's ability to withstand significant deformations is due to the integration of hydrogels as stretchable and transparent ionic conductors. The use of hydrogels in this context not only provides stretchability but also transparency, which aligns with the demand for advanced electronics that can withstand wear and tear.

The interconnected network of hydrogel frameworks can also mitigate issues related to electrolyte leakage, ensuring prolonged stability. Furthermore, the flexibility and deformability of hydrogels may enable their integration into various geometries, offering versatility in solar cell design. Overall, the 3D structure of hydrogels stands as a promising avenue for optimizing DSSC performance, addressing key challenges and paving the way for advancements in efficient and sustainable solar energy conversion.

2.5 Polyacrylamide Hydrogel-Based Solar Cell

The electric eel possesses remarkable electrical capabilities that allow it to operate with a peak electric potential of up to 600 V and currents of 1 A [3]. These abilities are made possible by thousands of ionic gradients arranged in series. Researchers have been inspired by this biological mechanism and have looked into using hydrogels, which can dissolve salts at various concentrations and display ion-selectivity through polyelectrolyte networks. By combining hydrogels with different ion concentrations or those with reverse ion selectivity, a tailored ionic gradient can be engineered. This innovative approach has the potential to generate electrical power in hydrogel systems using ionic gradients, similar to those observed in the electric eel. The use of hydrogels is a versatile and bio-

inspired method for developing new energy systems that can produce electrical power through controlled ion transport.

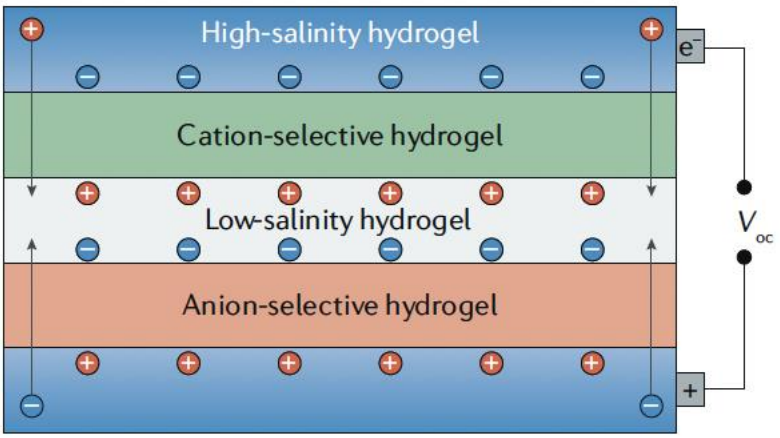


Figure 4 Artificial Electric Eel ([3] Schroeder, Thomas BH, et al. "An electric-eel-inspired soft power source from stacked hydrogels." Nature 552.7684 (2017): 214-218)

Schroeder et al. [3] introduced an innovative electric-eel-inspired power concept that harnesses ion gradients within miniature polyacrylamide hydrogel compartments, encapsulated by a repetitive arrangement of cation- and anion-selective hydrogel membranes. This artificial eel design involves stacking different hydrogels in sequence, namely a high-salinity hydrogel, a cation-selective hydrogel, a low-salinity hydrogel, an anion-selective hydrogel, and a second high-salinity hydrogel (as illustrated in Figure 4). When in contact, these hydrogels establish an ionically conductive pathway, creating an ionic gradient and generating an open-circuit voltage (Voc). The voltage output can be scaled up by stacking additional hydrogels in series, potentially reaching up to 110 V. An intriguing feature of this system is its departure from conventional batteries, as these hydrogel-based systems are soft, flexible, transparent, and hold the potential for biocompatibility. This work exemplifies the exciting possibilities of biomimicry in developing soft, bio-inspired energy systems with unique properties and applications.

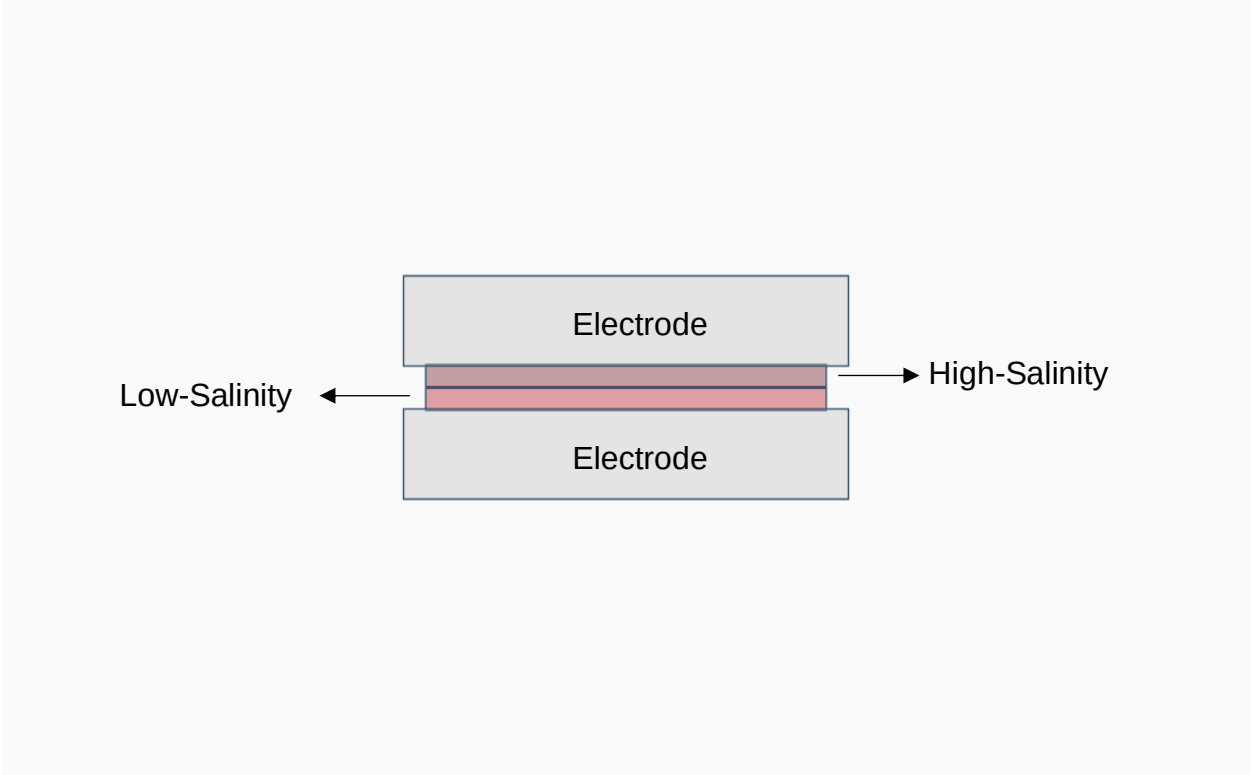


Figure 5 Polyacrylamide Hydrogel-based Solar Cell Structure

The concept of the artificial eel has inspired the development of a new structure for solar cells. This two-layered design is based on polyacrylamide hydrogel and aims to replicate the high-salinity and low-salinity layers observed in the artificial eel (as shown in Figure 5). By creating a similar depletion region using ions, instead of fixed charged atoms, the design aims to generate an open-circuit voltage (Voc) through the controlled modulation of ion concentrations. The hydrogel layers establish an ionic gradient upon contact, forming a dynamic and tunable ionically conductive pathway. This innovative approach to solar cell design introduces a novel strategy for developing ion-based photovoltaic systems, with the potential to enhance efficiency and performance.

Understanding the operational mechanisms of the polyacrylamide hydrogel solar cell requires an exploration of chemical thermodynamics. We need to understand how a concentration gradient creates a chemical potential that moves ions between the two layers, which is crucial in understanding how the device functions. Additionally, it's essential to delve into the concept of hydration radius, which explains how the radius of salt ions changes as they dissociate in the aqueous environment. By studying chemical

thermodynamics and ion behaviour, we can begin to uncover the intricate processes that govern the development of a potential difference across the layers of the polyacrylamide hydrogel solar cell.

Entropy (S) is a thermodynamic quantity that depends on internal energy (U), volume (V), and the number of particles (N). In thermodynamics, equilibrium is reached when U, V, and N are maintained at constant values. It's important to note that a system will have its maximum entropy when it's in equilibrium. According to the second law of thermodynamics, any system that's not in equilibrium will spontaneously try to move towards equilibrium. During this process, the system's entropy will progressively increase, which confirms the fundamental principle that systems tend to evolve in a direction that maximizes their disorder and randomness over time. A small change in S is defined as:

$$dS = \frac{1}{T}dU + \frac{P}{T}dV - \frac{u}{T}dN \quad (1)$$

where T: Temperature, P: Pressure, u: Chemical Potential.

Let's consider a closed and isolated adiabatic system with a fixed volume. This system is divided into two subsystems, namely subsystem 1 and subsystem 2. We assume that the internal energy and volume of subsystems 1 and 2 are fixed at their equilibrium values, $\overline{U}_1, \overline{V}_1$ and $\overline{U}_2, \overline{V}_2$, respectively. However, the number of particles in each subsystem is not in an equilibrium state value, $N_1 \neq \overline{N_1}$ and $N_2 \neq \overline{N_2}$.

We assume $N_1 + \Delta N_1 = \overline{N_1}$ and $N_2 + \Delta N_2 = \overline{N_2}$. Since the system is closed, particles could only transfer in between two subsystems, $\Delta N_1 = -\Delta N_2 \equiv \Delta N$. Entropy change in both subsystems can be found by integrating Eq. (1):

$$\Delta S_1 = \int_{N_1}^{N_1+\Delta N_1} dS_1 = \int_{N_1}^{N_1+\Delta N_1} \frac{1}{T}dU_1 + \frac{P_1}{T}dV_1 - \frac{u_1}{T}dN_1 \quad (2)$$

$$\Delta S_2 = \int_{N_2}^{N_2+\Delta N_2} dS_2 = \int_{N_2}^{N_2+\Delta N_2} \frac{1}{T} dU_2 + \frac{P_2}{T} dV_2 - \frac{u_2}{T} dN_2 \quad (3)$$

T is same for both subsystems as the system is adiabatic. As the internal energy and volume of each subsystem is constrained to a fix value $dU_1 = dU_2 = dV_1 = dV_2 = 0$. Eq. (2) & Eq. (3) simplifies to:

$$\Delta S_1 = -\frac{u_1}{T} \Delta N_1 = -\frac{u_1}{T} \Delta N \quad (4)$$

$$\Delta S_2 = -\frac{u_2}{T} \Delta N_2 = \frac{u_2}{T} \Delta N \quad (5)$$

With $\Delta S_{tot} = \Delta S_1 + \Delta S_2 \geq 0$ from second law of thermodynamics, we obtain:

$$\Delta S_{tot} = \frac{\Delta N}{T} (u_2 - u_1) \geq 0 \quad (6)$$

According to Eq. (6), the movement of ions between subsystems is caused by the difference in chemical potential of each subsystem. If $\Delta N < 0$, subsystem 1 will have a greater chemical potential than subsystem 2, and particles will move from subsystem 1 to 2. If $u_1 = u_2$, there will be no particle flow.

Understanding the particle flow between two systems with different particle concentrations is crucial. This flow happens due to the difference in chemical potential between the systems. To comprehend how ions behave when dissociated in aqueous solution is also necessary for the proper functioning of the device. When an ion dissolves in water, it attracts water molecules that surround it to form a shell (as shown in Figure 6). This process is called hydration. The distance from the center of an ion to the outer boundary of its hydrated shell in a solution is called the hydration radius. The hydration radius of an ion determines its mobility in solution. Ions with larger hydration radii tend to move more slowly than those with smaller radii because they are more heavily surrounded by water molecules.

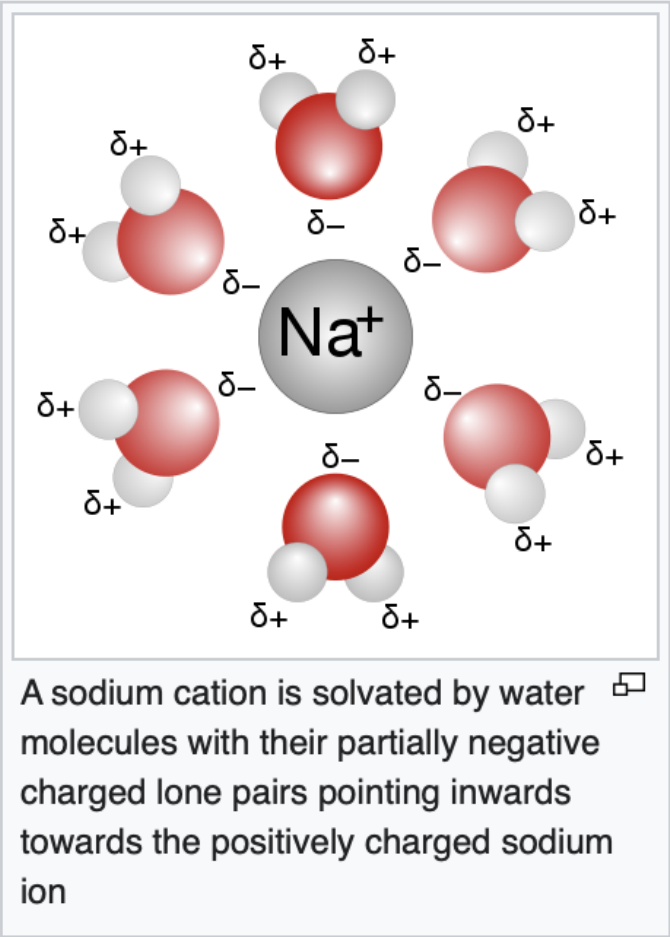


Figure 6 Sodium ion surrounded by water molecules (Source: Wikipedia)

Ions in a solution are surrounded by a protective layer of water molecules known as the solvation shell. The water molecules in the solvation shell form a coordinated arrangement around the ion where the negative ends are oriented towards positively charged ions, and the positive ends are oriented towards negatively charged ions. This arrangement is due to the electrostatic interactions between the charged ions and the partial charges on the water molecules. The number and orientation of water molecules in the solvation shell are determined by the size and charge of the ion. Smaller ions have more tightly bound solvation shells than larger ions. In summary, the solvation shell acts as a barrier, shielding the ion from other ions and molecules in the solution. The solvation shell plays a crucial role in the movement of ions in a solution. When an ion moves through the solution, it carries its solvation shell along with it. The size and structure of

the solvation shell can affect the ion's mobility, as well as its interactions with other ions and molecules in the solution. A thorough understanding of the solvation shell's properties is essential for predicting the behaviour of ions in solution.

The size of an ion's hydration shell, or the hydration radius, depends on the ion's size and the strength of its interaction with water molecules. Smaller ions tend to have larger hydration shells because water molecules can effectively surround them, while larger ions have smaller hydration shells. Figure 7 shows the hydrated ion size of NaCl when dissolved in water. The hydration radius of ions is influenced by their charge, which affects the strength of the electrostatic interaction between the ion and surrounding water molecules. A stronger electrostatic attraction results in a tighter and more compact hydration shell.

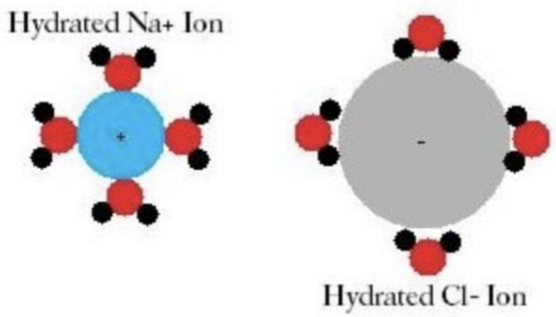


Figure 7 Hydrated Sodium (Na) & Chloride (Cl) ions (Source: Wikipedia)

The movement of ions in water is significantly influenced by their hydration. The hydration shell around an ion has a profound effect on its mobility and diffusion by displacing water molecules in its surrounding shell. This process is referred to as hydration shell drag. Ions with larger hydration shells experience greater drag as they move through water, slowing down their movement and increasing their effective size. This results in a higher hydrodynamic radius. As a result, ions with larger hydration shells have lower mobility and diffusion rates compared to smaller ions. Other factors such as temperature,

viscosity, and the presence of other solutes also influence the movement of ions in water. However, the hydration radius plays a crucial role in determining the extent to which ions can diffuse and interact with other molecules in solution.

i. Working Principles

The polyacrylamide (PAAm) hydrogel-based solar cell consists of a high-salinity (HS) hydrogel layer on top of a low-salinity (LS) hydrogel layer swelled with water containing a salt such as NaCl. When salt (NaCl) is added to water, it breaks down into positively charged sodium ions (Na^+) and negatively charged chloride ions (Cl^-). In the upper gel, there is a high concentration of these ions, while in the lower gel, the concentration is low (as shown in Figure 8). Initially, the device is neutral, with an equal number of Na^+ and Cl^- ions in each gel, and this is when there is no light exposure or voltage application. However, a concentration gradient exists for each ion, and this creates a difference in the chemical potential of the two layers of gel, which causes the ions to want to diffuse across the membrane.

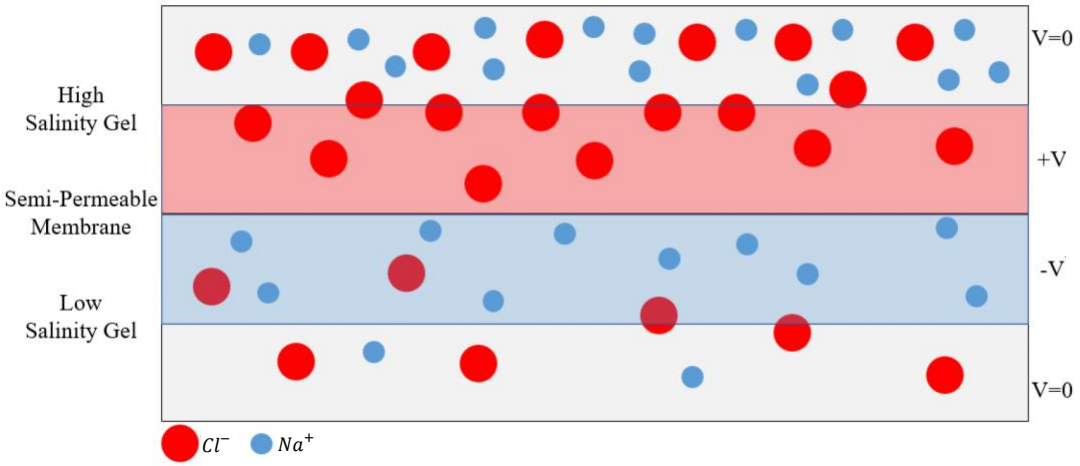


Figure 8 Polyacrylamide hydrogel-based solar cell at equilibrium

Establishing that the Cl^- ions are bigger than the Na^+ ions when hydrated. The Na^+ ions will have a higher probability of diffusion across the membrane than the Cl^- ions, due to their smaller hydration radius. This is referred to as Na^+ Diffusion Current. As more Na^+ ions diffuse, a negative charge builds up in the HS layer, and the positive charge gets

depleted from the HS layer. This generates a potential gradient (Na^+ Drift Current). With time, the potential difference becomes high enough to balance the Na^+ Diffusion Current and the Drift Current, resulting in dynamic equilibrium. The system then establishes a depletion region in the center as depicted in the Figure 8 by the shaded region.

In Figure 8, the Cl^- ions are attracted to the positive portion of the depletion region and tend to move across the membrane. However, their large size prevents them from diffusing. When the device is exposed to light, its temperature increases, which results in an increased rate of diffusion of all ions. This enables the Cl^- ions to move down their concentration gradient (Cl^- Diffusion Current) and in the direction of their electric potential difference (Cl^- Drift Current). The movement of these Cl^- ions is the photovoltaic current that is measured when the device is exposed to light as shown in Figure 9. Which represents a negative current, as by our convention, a positive current means that negative ions (Cl^-) are moving towards the positive probe (HS Layer).

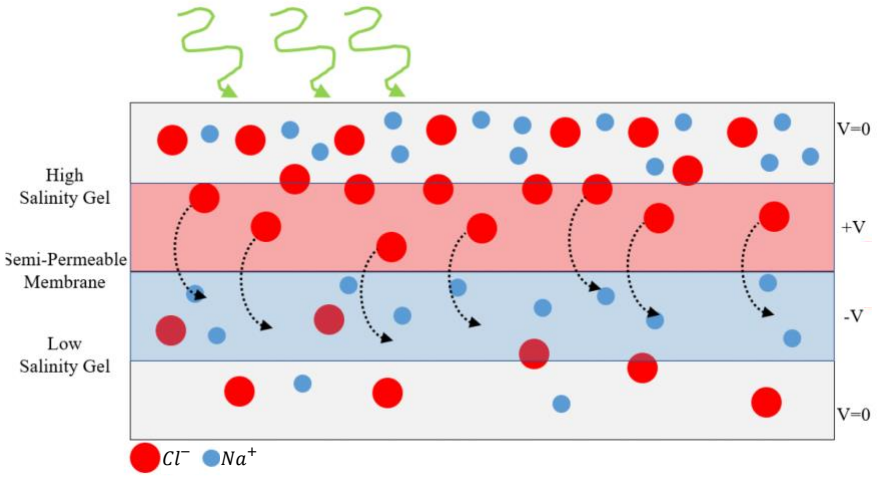


Figure 9 PAAm hydrogel-based solar cell upon illumination

ii. Limitations

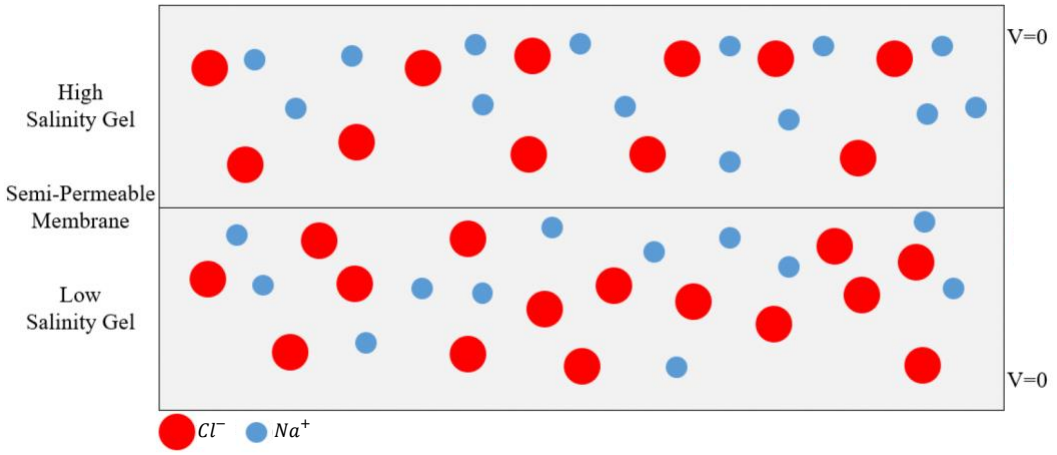
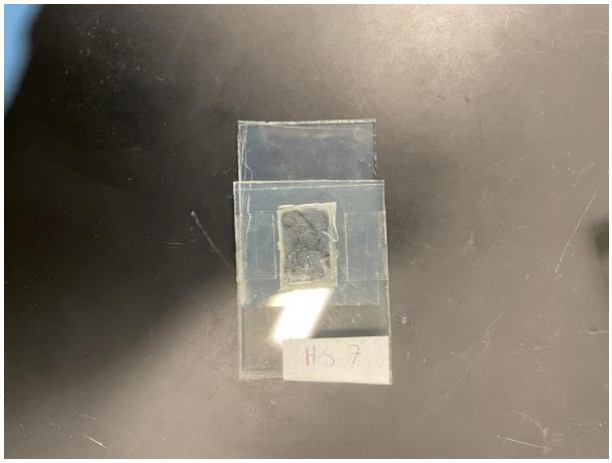


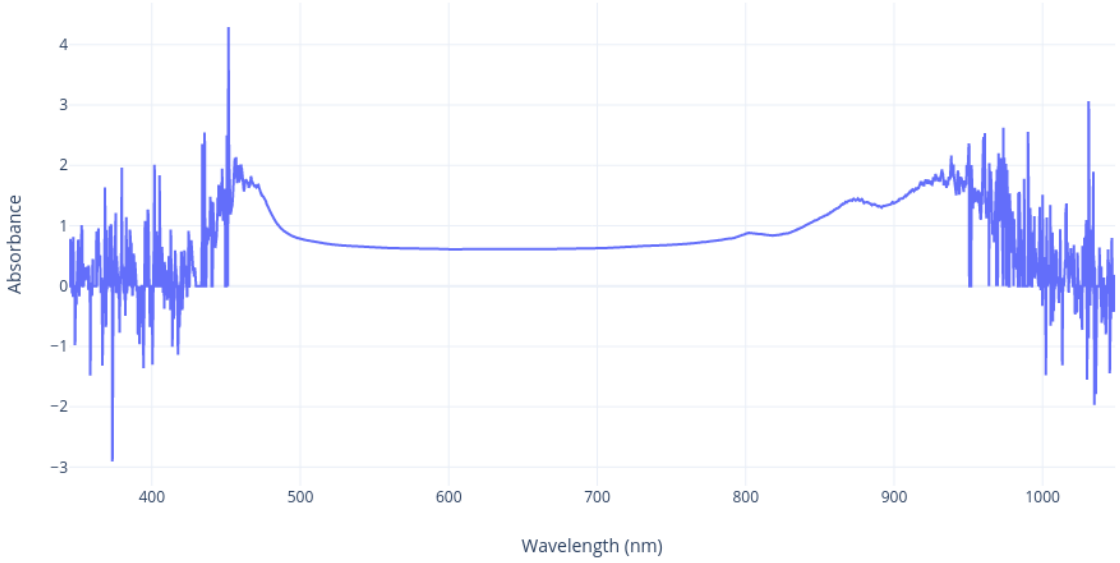
Figure 10 Neutralization of PAAm hydrogel-based solar cell

After some time of illumination, the ions however cannot move out of the hydrogel, so the photovoltaic current stops once the diffusion of Cl^- ions has neutralized the potential gradient as shown in Figure 10. Additionally, from the UV-Vis spectra presented in Figure 11b, it becomes evident that the hydrogel is transparent (as shown in Figure 11a) and does not absorb anything in the visible range. Hydrogels, being water-based, can only absorb in the far infrared range. However, thermal photons just increase the kinetic energy of particles. Therefore, thermal absorption only enhances the rate at which a system returns to its equilibrium state (minimal potential energy). This can only release potential energy that is already present (e.g., concentration gradient) but can never regenerate the potential (non-continuous, burst of energy release). If the potential energy of the system was continuously regenerated, the net power would be zero (e.g., replenishing the concentration gradient) because the energy being supplied is all that can be released.

Therefore, photoactive compounds must be added to hydrogels. Luminescent absorption converts an incident photon into potential energy that the system can actively harness to repeatably generate power through the motion of the exciton. There must be a probable path for the photo-exciton to take through the external load. Otherwise, energy loss will occur through recombination. The most efficient way of doing this would be to have a



(a)



(b)

Figure 11 a) Picture of PAAm Solar Cell. b) UV-Vis Spectra of PAAm Solar Cell

material next to the photoactive compound that is in resonance with the energy level of the exciton. This material would need discrete energy levels, the ability to conduct the photo-exciton, and the ability to connect to the external load. A semiconductor material would be the most efficient for this purpose. This would ensure the highest rate of energy transfer. Therefore, all photoactive compounds must be in proximity to a semiconductor material that is connected to the external load. Hydrogels do not allow electrons to flow across their barriers. This means that a DC electrical current cannot be sustained across

a hydrogel. Therefore, electrons must be moved across the hydrogel through redox transport. An electrolyte must be oxidized at one end of the material and reduced at the other for an electron to traverse the hydrogel.

Given the limitations of PAAm hydrogel-based solar cell, the only possible way of producing a hydrogel-based solar power generator is by making a device that resembles a DSSC, but with a hydrogel electrolyte as shown in Figure 12.

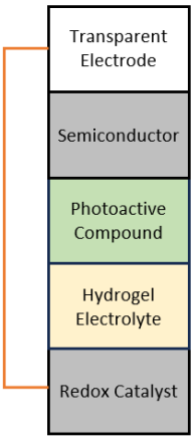


Figure 12 Proposed Structure

2.6 Dye-Sensitized Solar Cell (DSSC)

The working principle of DSSC involves four basic steps: light absorption, electron injection, transportation of carrier, and collection of current. The following steps are involved in the conversion of photons into current (as shown in Figure 13):

1. When exposed to sunlight, the sensitizing dye molecules absorb photons, initiating an electron excitation process. This leads to the generation of excitons (electron-hole pairs), which causes the electrons to be promoted from the ground state (S) to the excited state (S^*) of the dye.

$$(S) + hv \rightarrow (S^*)$$

2. The excited electrons are now injected into the conduction band of a semiconductor layer, which is below the excited state of the dye. While the holes remain in the dye. The excited electrons have a lifetime in the nanosecond range [26]. The semiconductor, acts as an electron transport medium, facilitating the movement of electrons towards the electrode. The semiconductor also absorbs a small portion of the photons from the UV range due to its wide band gap. The dye is consequently oxidized.

$$(S^*) \rightarrow (S^+) + e^-$$

3. The injected electrons are transported between the semiconductor layer and diffuse toward the conducting surface (electrode). The electrons reach the counter electrode, through the external circuit.

4. The electrolyte, typically composed of an iodide/triiodide redox couple dissolved in a liquid or embedded in a hydrogel, plays a pivotal role in completing the circuit by replenishing the dye with electrons and transferring the charge to the counter electrode. The electrons at the counter electrode reduce I_3^- to I^-; thus, dye regeneration or the regeneration of the ground state of the dye takes place due to the acceptance of electrons from I^- ion redox mediator, and I^- gets oxidized to I_3^- (oxidized state).

$$(S^+) + e^- \rightarrow (S)$$

5. The oxidized mediator (I_3^-) diffuses towards the counter electrode and reduces to I^- ion.

$$I_3^- + 2e^- \rightarrow 3I^-$$

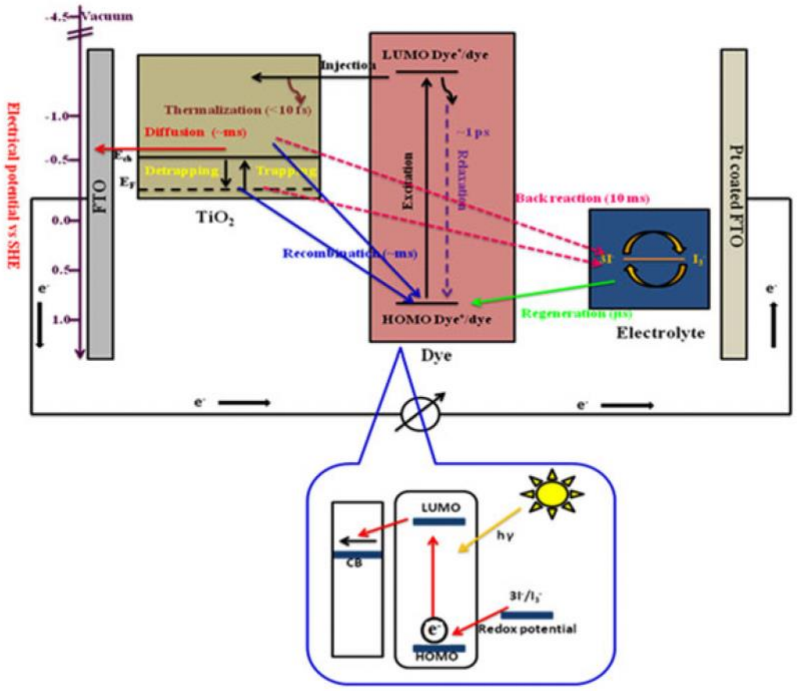


Figure 1. Schematic of all reactions that occur inside a DSSC with highest occupied molecular orbital-lowest unoccupied molecular orbital (HOMO-LUMO) energy levels and with corresponding electrical potential vs standard hydrogen electrode (SHE). FTO, fluorine doped tin oxide.

Figure 13 [27] Shalini, S., et al. "Status and outlook of sensitizers/dyes used in dye sensitized solar cells (DSSC): a review." International journal of energy research 40.10 (2016): 1303-1320.

This movement of charge results in the creation of an electric current that can be harvested for practical use.

i. Photoanode

The photoanode is a crucial component responsible for absorbing light and initiating the photovoltaic conversion process. Typically composed of a transparent conductive substrate, a layer of wide-bandgap semiconductor material, and a sensitizing dye, the photoanode facilitates the absorption of photons and the generation of electron-hole pairs. A high electron transport rate is required to reduce electron–hole recombination rate and enhance the conversion efficiency.

Transparent and Conductive Substrate: DSSCs are typically made of two sheets of transparent, conductive materials that serve as both current collectors and a substrate for the deposition of the catalyst and semiconductor. There are two essential qualities of a substrate for a DSSC: First off, the substrate needs to be more transparent than 80% in order to allow the best sunlight to reach the cell's active region. Second, it should have a high electrical conductivity for effective charge transfer and decreased energy loss in DSSCs. Tin oxides with fluorine and indium doping (FTO, SnO2: F and ITO, In2O3: Sn, respectively) are frequently used as conductive substrates in DSSCs. These substrates are made of soda lime glass that has been covered with layers of indium- and fluorine-doped tin oxide.

Despite their excellent resistance to oxygen and water, their practical applications are limited by their high cost, fragility, rigidity, and shape restrictions. Additionally, this system cannot be produced via the roll-to-roll method. Flexible substrates that are lightweight and have good portability have emerged as a substitute. Conductive plastics, such as ITO-coated polyethyleneterephtalate (ITO/PET) and ITO-coated polyethylenenaphtalate (ITO/PEN), are one type of flexible substrate [28]. Since their maximum withstandable temperature is only about 150°C, the production of the TiO_2 layer at low temperatures presents the biggest problem for conducting polymers. In order to achieve good electrical contact between particles, the TiO_2 layer is often sintered at higher temperatures of 400–500°C. Furthermore, the normal TiO_2 paste contains viscous solvents and an organic binder that should be eliminated during a high-temperature sintering process. To avoid using the high-temperature sintering procedure, mechanical compression of nanocrystalline semiconductor powder and hydrothermal production of metal oxide nanocrystals have been proposed [28].

Metal foils, such as titanium, zinc, and stainless steel foils, are another type of flexible substrates that naturally have excellent conductivity, light scattering, and high-temperature sintering properties. The Ti foil-based DSSC is the best among them due to its qualities of greater conductivity and enhanced corrosion resistance that are brought about by the presence of a passive coating of TiO_2 on the surface of a Ti foil. Two

significant obstacles must yet be solved for metal-based DSSCs, though. The relevant DSSCs must be lit from the backside because metal substrates are opaque. Because the Pt counter electrode partially reflects light and the iodine in the electrolyte absorbs photons in the near UV range, there is a loss of around 25% of the incident solar energy [28]. Second, after sintering, there would be significant metal oxide development, which would increase interfacial resistance and lower cell performance [28].

Huabo, et al. [29], fabricated an electrode through the in situ polymerization of aniline within an acidic aqueous solution of polyvinyl alcohol (PVA), coupled with the freezing-thawing method. This approach resulted in the creation of a reinforced conducting polymer hydrogel, specifically the polyaniline/polyvinyl alcohol (PANI/PVA) hydrogel, which exhibited a distinctive combination of attributes. These included a hierarchical nanoporous microstructure, mechanical integrity, and commendable capacitive behaviour. The PANI/PVA hydrogel was directly employed as a self-supported electrode material, presenting a novel strategy for constructing high-performance electrodes in various applications. This work not only demonstrated the feasibility of this fabrication method but also opened avenues for further exploration into the development of advanced electrode materials with enhanced properties.

A supramolecular strategy was developed to prepare conductive hydrogels capable of producing hydrogels with exceptional mechanical and electrochemical characteristics. The supramolecular assembly of polyaniline and polyvinyl alcohol through dynamic boronate bond yields the polyaniline–polyvinyl alcohol hydrogel (PPH), which shows remarkable tensile strength (5.3 MPa) and electrochemical capacitance (928 F/g) [30].

Working Electrode (WE): On a transparent conducting glass plate formed of FTO or ITO, the working electrodes (WE) are created by depositing a thin layer of oxide semiconducting materials such as TiO_2, Nb_2O_5, ZnO, SnO_2 (n-type), and NiO (p-type). These mesoporous oxides provide a large contact area between dye and semiconductor which allows better electron transferring through the DSSC. The energy band gap of these oxides ranges from 3 to 3.2 eV. Due to its greater energy band gap of 3.2 eV

compared to a rutile form's band gap of around 3 eV, anatase allotropic TiO_2 is more noteworthy for use in DSSCs, while alternative wide band gap oxides like ZnO and Nb_2O_5 have also shown promising results [26].

TiO_2 crystals are divided into rutile, brookite, and anatase. The two primary crystalline forms of titanium dioxide are anatase and rutile; however, brookite TiO_2 is extremely rare and is only stable at temperatures above 600 °C. Additionally, 4% of incident light in the near-UV region is absorbed by rutile TiO_2, producing holes that would lower the long-term stability of DSSCs [5]. As a result, anatase TiO_2 is ideal for the semiconductor layer on the DSSC photoanode. Since TiO_2 has a high dielectric constant for anatase, the injected electron is effectively electrostatically shielded from the oxidized dye molecule, preventing any recombination before the dye molecule is reduced by the electrolyte. TiO_2 high refractive index for anatase results in efficient diffuse scattering of light inside the porous photoanode and hence significantly enhances the light absorption.

The film's ability to function as a sensitized photoanode was enhanced by applying a layer of pure TiO_2 through $TiCl_4$ treatment [31]. This process effectively covers the impurities and improves both the injection efficiency and blocking properties of the semiconductor-electrolyte junction. Khannam, Momina, et al. [32], studied DSSCs that use GO@TiO_2 nanocomposite photoanodes. After testing various concentrations, it was found that the optimal GO content was 2.5 wt%. The DSSCs with this concentration showed a Jsc of 7.67$mA\ cm^{-2}$, a Voc of 0.76V, and a photo conversion efficiency of 3.97%. This efficiency was significantly higher than that of DSSCs using pure TiO_2 nanoparticles.

These working electrodes are then submerged in a solution that contains a combination of a photosensitive molecular sensitizer and a solvent because these semiconducting layers only absorb a small portion of light in the UV region. The dye is covalently bound to the TiO_2 surface after the film has been immersed in the dye solution. Due to the electrode's huge surface area and highly porous shape, a lot of dye molecules adhere to the nanocrystalline TiO_2 surface, increasing light absorption at the semiconductor surface.

The device's fill factor (ff) and open-circuit voltage (Voc) can be remarkably improved by dipping the working electrode into 4-tert-butylpyridine. This enhancement does not significantly affect the short-circuit photocurrent (Jsc). The boost in the open-circuit voltage and fill factor is due to the suppression of dark current at the semiconductor electrolyte junction. The reduction of triiodide by conduction band electrons causes the dark current, despite the TiO_2 surface being covered by a monolayer of dye. The triiodide can cross the dye layer or enter nanometer-sized pores, where the dye cannot penetrate, leaving the TiO_2 surface exposed to redox electrolyte. The use of 4-tert-butylpyridine slows down the triiodide reduction rate.

Photosensitizer (Dye): Dye is the component of DSSC responsible for the maximum absorption of the incident light. Any material being dye should have the following photophysical and electrochemical properties [26]:

1. The dye must first be luminous.
2. The dye's absorption spectrum should include both near-infrared (NIR) and ultraviolet-visible (UV-vis) regions for maximum absorption of light.
3. The lowest unoccupied molecular orbital (LUMO) should be placed as close to the surface of the TiO_2 as possible and should be higher with respect to the TiO_2 conduction band (CB) potential. The highest occupied molecular orbital (HOMO) should be placed far from the surface of the TiO_2 to avoid the recombination of a hole in HOMO with an electron in CB of TiO_2.
4. To ensure easy electron transfer from electrolyte to dye, the HOMO should be located below the redox electrolytes.
5. To increase the long-term durability of cells, the dye's perimeter should be hydrophobic. This minimizes direct contact between the electrolyte and the anode and prevents water from distorting the dye from the TiO_2 surface, which could lower cell stability.
6. Co-absorbents such chenodeoxycholic acid (CDCA) and anchoring groups like alkoxy-silyl, phosphoric acid, and carboxylic acid group were placed between the

dye and TiO_2 to prevent the dye from aggregating over the TiO_2 surface. Due to the inhibition of dye aggregation, the recombination interaction between the redox electrolyte and the electrons in the TiO_2 nanolayer is constrained, and stable linkage is created as a result.

7. The dye should have functional groups such as –COOH, –PO3H2, and –B(OH)2 for stable adsorption onto the semiconductor substrate [33].

DSSC currently employs various types of sensitizers, including inorganic ruthenium (Ru)-based dyes, metal-free organic dyes, quantum-dot sensitizers, perovskite-based sensitizers, and natural dyes. The use of metal-free, quantum-dot, perovskite-based, and natural dyes has become more popular due to their affordability, ease of preparation, accessibility, and eco-friendliness. However, these alternatives have generally been found to be less effective than Ru-based dyes due to their limited absorption range (Δλ≈100–250 nm), negative dye aggregation, and instability.

For DSSCs, which can achieve solar-to-electricity conversion efficiencies of around 11% under AM 1.5 conditions due to the favourable photoelectrochemical properties as well as the excellent chemical stability and intense light absorption over a wide visible range, the metal-based sensitizers composed of chromophores of ruthenium complexes have been extensively studied.

In 1993 Nazeeruddin et al. [31], the conversion efficiency of 10.3% was reported using Ru dye (N3 dye) as sensitizer (N3-cis-di (thiocyanato) bis(2,2-bipyridine-4,4-dicarboxylate) ruthenium). Later in 2005 Nazeeruddin et al. [34], a new dye called N179 was developed (di-tetrabutyl ammonium cis-bis (isothiocyanato) bis (2,2′-bipyridyl-4,4′-dicarboxylato) ruthenium (II)), which was similar to N3 but resulted in a conversion efficiency of 11.2%.

A sample list of the photovoltaic characteristics for DSSCs using complicated photodyes based on Ru is provided in Table 1. The disadvantage of ruthenium complex dyes is that

they contain heavy metal which is expensive and harmful to the environment. Therefore, metal-free organic dyes are used as alternatives.

Table 2 A partial list of the photovoltaic parameters for the dye-sensitized solar cells (DSSCs) using Ru-based complex dyes as the sensitizer

Ru complex sensitizer	V_{OC} *(V)*	J_{SC} *(mA/cm²)*	*FF (%)*	*η (%)*
cis-[Ru([a]$dcbH_2$)$_2$(NCS)$_2$]	0.64	5.0	76	10.4
N719	0.85	17.7	75	11.1
N621	0.78	16.8	73	9.6
Black dye	0.74	20.9	72	11.1
cis-[Ru([a]$dcbH_2$)$_2$(NCS)$_2$]	0.70	15.0	74	7.8
[Ru([a]$dcbH_2$)$_2$([b]acac)]Cl	0.67	13.2	68	6.0
Ru([c]bmipy)([d]bpy-PO_3H_2)(NCS)	0.60	8.6	70	4.1
[Ru([a]$dcbH_2$)$_2$([e]phdmp)]Cl_2	0.42	0.60	38	3.8
Ru(bpy-$(CH_2OH)_2$)$_2$(NCS)$_2$	0.51	10.0	48	3.8
Ru([a]$dcbH_2$)$_2$([f]qdt)	0.60	11.1	70	3.7
[Ru([a]$dcbH_2$)$_2Cl_2$]	0.57	2.6	38	2.1
[Ru([a]$dcbH_2$)$_2$([g]aphb)]	0.58	5.5	48	1.5

[a]$dcbH_2$ = 4,4′-(CO_2H)2-2,2′-bipyridine
[b]acac = acetoacetonate
[c]bmipy = benzimidazol
[d]bpy = bipyridine
[e]phdmp = pteridinedione
[f]qdt = quinoxaline-2,3-dithiolate
[g]aphb = phenanthrolin-5-yliminomethyl-phenol.

Table 1 [4] L.-Y. Lin and K.-C. Ho, "Dye-sensitized solar cells," Encyclopedia of Modern Optics, pp. 270–281, 201

The metal-free organic dyes are relatively inexpensive, since they can be easily synthesized, and their resources are more abundant than that of the noble metals. Secondly, the extinction and absorption coefficients of organic dyes are relatively higher than those of the noble metal-based ones.

ii. Electrolyte

The electrolyte is a crucial part of the dye regeneration after electron injection and the electron transfer between the photoanode and the CE. The electrolyte can be classified into liquid electrolyte, quasi-solid-state electrolyte, and solid-state electrolyte. The following properties should be present in an electrolyte [26]:

1. Redox couples should be able to regenerate the oxidized dye efficiently.
2. Should have long-term chemical, thermal, and electrochemical stability.
3. Should be non-corrosive with DSSC components.

4. Should be able to permit fast diffusion of charge carriers, enhance conductivity, and create effective contact between the working and counter electrodes.
5. The absorption spectra of an electrolyte should not overlap with the absorption spectra of a dye.

Additives, solvents, and redox couples make up the liquid electrolyte. The photoanode and CE charges are transferred by the redox couple, who are also in charge of dye regeneration. The redox couple has a redox potential that is less negative than the sensitizer's oxidised state. In addition, the redox couples require fast electron transfer kinetics at the CE, slow electron recombination kinetics at the sensitizer, minimal visual absorbance, noncorrosive, moderate stability, and good diffusion characteristics.

I^-/I_3^- has been demonstrated as a highly efficient electrolyte, but there are certain limitations associated with its application in DSSCs. I_3^- is extremely corrosive toward metals such as copper or silver, and a significant part of visible light would be absorbed by the I^-/I_3^- based electrolyte. A recorded efficiency of 12.3% was attained for the DSSC with Co (II/III) tris(bipyridyl)-based redox couple in its electrolyte. On the other hand, the additives were used in the electrolyte to enhance the photovoltaic performances. Specific cations like guanidium or alkali cations are typically used to increase the photocurrent density. The cations in the electrolyte would adsorb on the surface of the semiconductor layer to render the conduction band of the semiconductor shift toward more positive potentials, thus affecting the electron injection dynamics of the dye molecules in the excited state. Also, nitrogen-containing heterocyclic compounds like 4-tert-butylpyridine (4-TBP) and pyridine analogs of the N-alkylbenzimidazole derivatives are purposely used to improve the Voc [35].

The selection of solvents for the liquid electrolyte typically are organic solvents and ionic liquids. Among these, commonly used organic solvents include acetonitrile (ACN), ethylene carbonate (EC), 3-methoxypropionitrile (MPN), propylene carbonate (PC), N-methylpyrrolidone (NMP), and even water. Organic solvents and conducting salts make up organic electrolytes. These electrolytes are preferred in the commercial market due to

their high voltage window. Compared to aqueous electrolytes, organic electrolytes have a voltage range of up to 3.5V. Acetonitrile and propylene carbonate are commonly used as solvents in organic electrolytes. Although acetonitrile can dissolve large amounts of salts, it poses environmental and toxic concerns. On the other hand, propylene carbonate is environmentally friendly, conductive, and can operate at high temperatures with a larger electrochemical potential window. However, the biggest drawback allied with the ionic liquid is its leakage factor. Thus, solid-state and quasi-solid-state electrolytes are developed to avoid the drawbacks associated with ionic liquid (IL) electrolytes.

The solid-state DSSC applied the hole transport materials (HTMs) or the solid-state electrolyte containing I^-/I_3^- redox couple as the medium to solve the solvent leakage and corrosion issues. The field of conducting polymer in DSSCs is making slow progress due to deposition difficulties caused by the solid polymer's inability to penetrate the TiO_2 nanoporous layer. This has resulted in limited use of conducting polymers in DSSCs, despite their potential in addressing corrosion issues.

The quasi-solid-state electrolyte consists of a polymer network swollen with liquid electrolytes or ionic liquid electrolytes. Since the quasi-solid-state electrolyte has both a solid's cohesive characteristic and a liquid's diffusive transport property, it has greater long-term stability than liquid electrolytes.

Nath, Bikash Chandra, et al. [36], fabricated DSSC using PVA/MWCNT/PANI based gel electrolyte. This gel was stable up to 250° C and achieved a conversion efficiency of 2.18%. The overall current density of the DSSC was increased by the addition of MWCNT. Karakuş, Mücella Özbay, et al. [37], investigated the network structure effect of hydrogels on DSSC performance, used as quasi-solid-state electrolytes using different amounts of crosslinking between the polymer chains. The increased amount of crosslinking during synthesis raised conductivity. However, it was observed that the conversion efficiency of DSSCs does not follow the rising trend in conductivity with increased cross-linking. Crosslinking also affects the absorption of the liquid electrolyte by the hydrogel.

iii. Counter electrode (CE)

To regenerate the sensitizer after electron injection and produce the photocurrent, the CE reduces the oxidized redox couple utilized as a mediator in the external circuit by moving electrons from the external circuit to the electrolyte. Important requirements for a CE of DSSCs include strong electrocatalytic activity, outstanding electrical and thermal conductivities, high corrosion resistance, wide electrochemical surface areas, high exchange current densities, and low charge transfer resistances. Platinum (Pt) or carbon (C) are typically used in the preparation of CE in DSSCs. The counter electrode collects holes from the hole transport materials (HTMs) and catalyzes the reduction of I^-/I_3^- liquid electrolyte. Pt has a better efficiency and is typically employed as a counter electrode, however because of its higher cost and lower availability, Pt has to be replaced.

To reduce the production cost of the cells, cheaper materials were proposed. Conducting polymers like poly(3,4-ethylenedioxythiophene) (PEDOT), PEDOT doped with poly (4-styrene sulfonate) (PEDOT:PSS), polypyrrole (PPy), polyaniline (PANI), and poly(3,4-propylenedioxythiophene) (PProDOT) have been used as the catalyst on the CE of DSSCs, due to their unique properties such as high conductivity, low cost, good stability, and high catalytic activity for I_3^- reduction. Due to its simple synthesis, strong conductivity, outstanding environmental stability, and intriguing redox characteristics, PANI has received the greatest research attention among conducting polymers in recent years. The performance of the conducting polymer can be enhanced by designing the morphology to achieve optimized surface roughness or doping foreign anions such as SO_4^{2-}, ClO_4^-, BF_4^-, Cl^-, and $tosyl^-$ into the conducting polymer film to increase the conductivity. However, the major problem of the conducting polymer is that the thick layer is required to achieve sufficient catalytic activities.

Carbon materials like graphene, glassy carbon, and carbon nanotubes (CNT) are also interesting low-cost alternatives to Pt. These materials have the advantages of high heat resistance, high electronic conductivity, high electrocatalytic activity toward I_3^- reduction, and high corrosion resistance. However, it is important to note that carbon-based CE

requires a large dosage to achieve the desired catalytic activity and there may be issues with the connection between the carbon film and the substrate.

Li, Qinghua, et al. [38], substituted PANI for Pt to construct the counter electrode for DSSC. The PANI counter electrode, which had a microporous structure and a diameter of approximately 100 nm, exhibited lower charge-transfer resistance and superior electrocatalytic activity for the I^-/I_3^- redox reaction than Pt electrode. As a result, the DSSC with PANI counter electrode attained an overall energy conversion efficiency of 7.15%, surpassing that of the DSSC with Pt counter electrode.

Zhang, D. W., et al. [39], synthesized graphene nanosheets (GN) and used them as a substitute for platinum as counter electrode. GN counter electrodes were developed by annealing GN films at different temperatures. The annealed GN films presented a unique 3D network structure which enhanced charge transfer reaction within electrolyte by enlarging effective reaction area and ensuring good adhesion of GN catalysts to FTO substrates. The performance of DSSCs with Pt-based and GN-based counter electrodes fabricated under the same conditions was comparable. An overall conversion efficiency of 6.81% was achieved by GN-based counter electrode DSSC.

Tao, Yulun, et al. [40], fabricated TiO_2/PANI/Graphene-PVA hydrogel (TPGH) by combining TiO_2/PANI/Graphene powder with polyvinyl alcohol (PVA) hydrogel to be used as photocatalyst. It was shown that by introducing PANI the system promoted the separation of photogenerated electron-hole pairs. In composites, graphene functions as an electron acceptor for photogenerated electrons. This helps prevent carrier recombination and boosts charge transfer. When combined with PANI, graphene leads to a substantial increase in photocurrent when exposed to visible-light irradiation. The significant boost in photocurrent indicates that electron-hole pairs can be efficiently separated and utilized in the presence of both PANI and graphene.

2.7 Evaluation of DSSC Performance

Like other solar cells, the performance of the DSSC can be evaluated by using the open-circuit voltage (V_{oc}), the short-circuit current density (J_{sc}), the fill factor (FF), the solar-to-electricity conversion efficiency (η), the incident photon-to-current conversion efficiency (IPCE), and the charge transfer resistances measured by using the electrochemical impedance spectroscopy (EIS).

V_{oc} is determined by the difference in energy of the electron at the semiconductor and the CE for a typical photoelectrochemical cell, or the difference in energy level of the quasi-Fermi level of the semiconductor under illumination and the Nernst potential of the electrolyte solution. V_{oc} is measured with no current flow and is the maximum voltage which the DSSC can provide to an external circuit. Eq. (7) shows the relation of photovoltaic parameters to V_{oc} for regenerative photoelectrochemical systems.

$$V_{oc} = V_T \ln\left(1 + \frac{J_{sc}}{J_o}\right) \quad (7)$$

where V_T is the thermal voltage and J_o is the reverse saturation current density.

J_{sc} is the maximum output current of a DSSC and is measured under illumination at the zero voltage across the cell. The magnitude of J_{sc} is determined by the product of the optical absorption efficiency, charge collection, and the solar irradiance integrated over the whole wavelengths of the incident light spectrum, as shown in Eq. (8).

$$J_{sc} = e \int (1 - 10^{-Abs(\lambda)}) IQE(\lambda) \phi(\lambda) d\lambda \quad (8)$$

where Abs(λ) is the absorbance of the sensitizer as a function of the wavelength λ, e is the elementary electron charge, and $\phi(\lambda)$ is the standard AM 1.5 irradiance spectrum. IQE(λ) is the internal quantum efficiency for the hot electron injection, dye regeneration, and then charge collection.

FF is defined as the ratio of the maximum power output (P_{max}) from a DSSC to the product of V_{oc} and J_{sc}. The fill factor can be calculated by using Eq. (9).

$$FF = \frac{P_{max}}{V_{oc}\, J_{sc}} = \frac{V_{max}\, J_{max}}{V_{oc}\, J_{sc}} \quad (9)$$

where $V_{max}\ and\ J_{max}$ respectively represent the photovoltage and photocurrent density corresponding to P_{max}.

The η of a DSSC is calculated as the ratio between the maximum generated power (P_{max}) and the incident power (P_{in}). The incident power is equal to the irradiance of the AM1.5 spectrum normalized to 1000W/m^2. Hence, the η of a DSSC can be determined by the V_{oc} , J_{sc} , FF, and P_{in} as shown in Eq. (10) as follows.

$$\eta = \frac{P_{max}}{P_{in}}.100\% = \frac{V_{oc}\, J_{sc} FF}{P_{in}}.100\% \quad (10)$$

IPCE is defined as the ratio of the number of photo-generated electrons ($N_{electrons}$) flowing in the external circuit to the number of incident photons ($N_{photons}$) with a given wavelength. IPCE is also referred to as the external quantum efficiency (EQE). IPCE or EQE value is most often expressed as the percentage of the absorbed incident photons and the converted electrons as a function of the wavelength. The internal quantum efficiency (IQE) is also reported which represents the number of absorbed photons converted to electrons and indicates how efficiently the numbers of absorbed photons are converted into current.

$$IPCE(\lambda) = IQE(\lambda).LHE(\lambda) \quad (11)$$

$$LHE(\lambda) = \left(1 - 10^{-Abs(\lambda)}\right) \quad (12)$$

where LHE(λ) is the light-harvesting efficiency.

Only a small amount of information regarding the electron transport and recombination rates may be obtained from the steady state J-V measurements. Therefore, to examine the charge transfer kinetics and therefore learn about the resistance and capacitance of various DSSC components, a dynamic technique like the Electrochemical Impedance Spectroscopy (EIS) is needed. The series resistance (RS), the recombination resistance at the semiconductor/dye/electrolyte interface (Rct1), the electron transfer resistance in the CE (Rct2), and the diffusion resistance of the electrolyte (Zw) causes are the four main investigated resistances at the interfaces of DSSCs from the charge transfer processes.

i. Model of a Solar Cell

Understanding the electrical behavior and performance of DSSCs requires an exploration of their equivalent model circuit. This circuit model is a representation of the intricate interplay of electrical components within a DSSC system. It simplifies the complex electrochemical processes inherent to DSSCs into a set of interconnected electrical elements, serving as a conceptual framework. To delve into this equivalent model circuit, one needs to understand the roles of resistances, capacitances, and other parameters. This offers insights into how the various components collaborate to determine the overall electrical response of a DSSC. This lays the groundwork for the optimization and advancement of these photovoltaic devices.

Under dark conditions, the I-V characteristics of a DSSC resemble that of a diode (PN junction), as shown in Figure 14b by dotted line. When an illuminated photovoltaic device is connected to a resistive load, a voltage appears across the PN junction due to the current passing through the load. This voltage decreases the built-in voltage of the PN junction, resulting in carrier injection and diffusion, similar to a diode. As a consequence, a forward diode current (J_D) emerges, in addition to the photo-generated current J_{ph}. The photocurrent passing through the load causes a potential drop across the load, which makes the diode forward-biased, resulting in a forward diode current in the opposite direction of the photocurrent. In Figure 14, the forward diode current is considered positive.

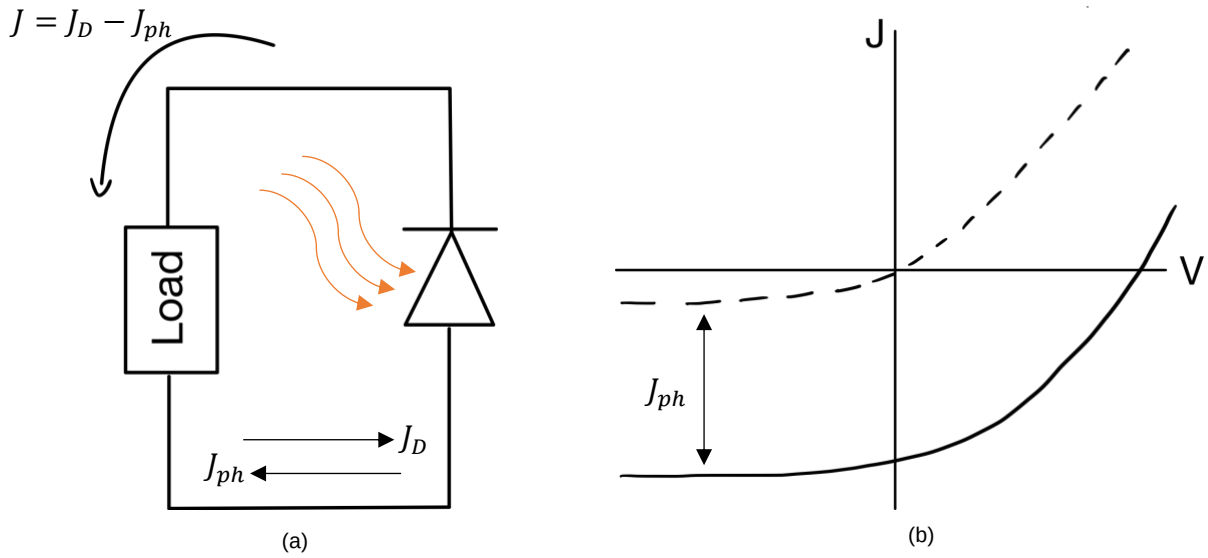


Figure 14: a) Equivalent circuit of a solar cell connected to a load. b) I-V of solar cell under dark & illuminated conditions

In simple terms, when we talk about devices operating in different quadrants, it's like understanding if they consume or deliver power. In the case of solar cells, they work in the fourth quadrant, and instead of using power, they generate it. To break it down, we can imagine a solar cell as having two main parts: one acts like a source of current (J_{ph}) from the sunlight it captures, and the other part acts like a diode that reduces the photocurrent in a specific direction when connected to a load (as shown in Figure 15a). This combination forms what we call an equivalent circuit model for an ideal solar cell. So, when we're looking at a solar cell, we're not just talking about a device that sits passively; it actively produces power from the sun. In solar cells, the operating point is determined by the load that's connected to it. The optimal operating point is where the device generates the highest power output. To achieve this, a buck-boost converter is used to operate the solar cell at the point where it produces maximum power. Figure 15b illustrates the operating point of a solar cell.

The series resistance (Rs) in a solar cell causes a voltage drop, which means that the ideal voltage the solar cell could provide gets a bit lost when we connect it to something that draws current, like a device or a load. Many factors influence this series resistance, such as the type of metal used for the electrode, how well the electrode makes contact, the thickness of the electrode, how much the semiconductor material is doped, and the

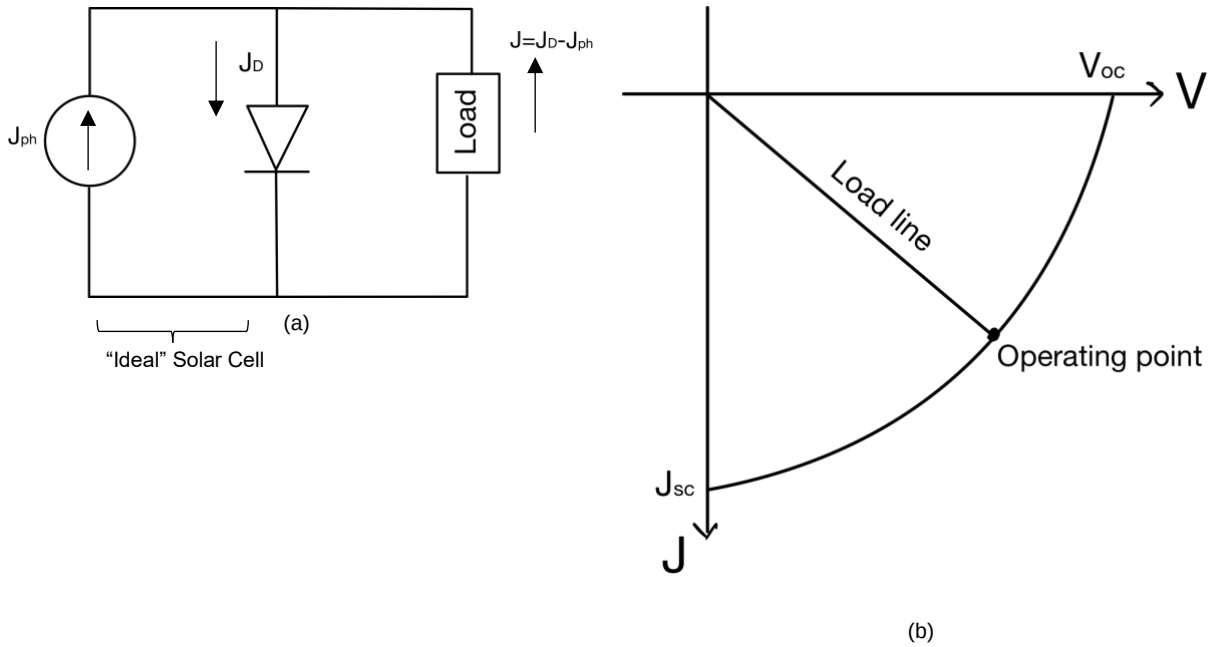


Figure 15: a) Ideal Solar cell model. b) Operating point of solar cell on illuminated IV.

size of the electrode's contact area. These resistances can be lumped together in a resistor connected in series with the ideal solar cell model (Figure 16a). Having a high series resistance can hurt the performance of the solar cell. As shown in Figure 16b, having more series resistance can reduce the maximum power that the solar cell can deliver. If the series resistance is very high, it can even put a limit on how much current the solar cell can provide in a short circuit situation.

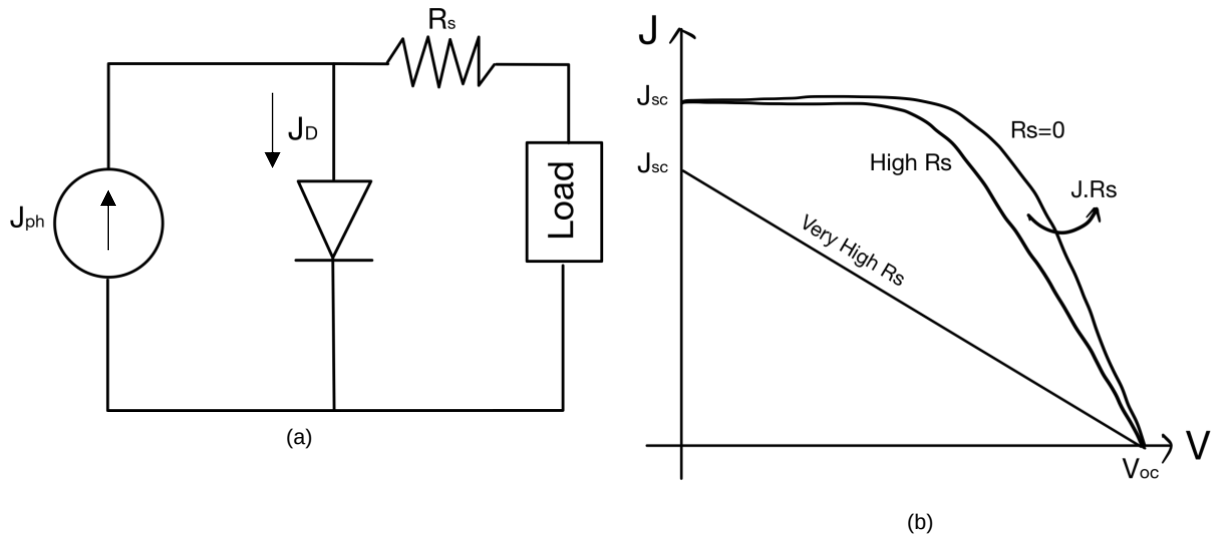
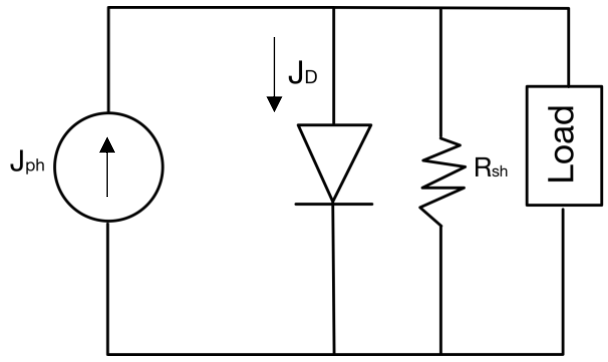
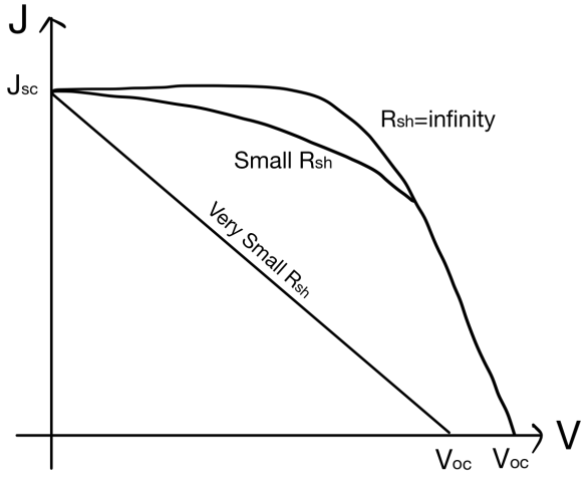


Figure 16: a) Equivalent circuit model of solar cell with series resistance effect. b) Effect of Rs on solar cell performance.

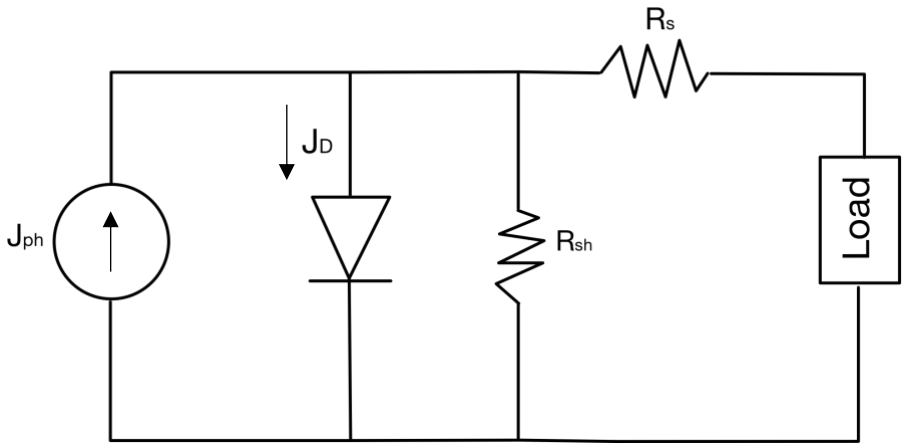
We have been assuming that the device has an infinite shunt resistance, but in reality, there is a finite shunt resistance. When a solar cell operates, a small fraction of the photo-generated carriers can flow through the device surfaces, edges, or grain boundaries (in the case of poly- or multi-crystalline materials). This process effectively shunts the solar cell. In an ideal case, the shunt resistance is expected to be infinite. However, material-related effects and device fabrication technology can cause shunt, for instance, non-uniform junctions and metal spiking from some points in the front contact grid, especially in ultra-shallow devices. These effects can be lumped into a resistor connected in parallel with the ideal solar cell as shown in Figure 17a (Note: here it is assumed that series resistance is negligible). Low shunt resistances, due to defects in materials or technology-induced shunt paths, tend to reduce the maximum power and efficiency. Much lower shunt resistances (less than 1 ohm) have a direct impact on the open circuit voltage (Figure 17b).



(a)



(b)



(c)

Figure 17: a) Solar cell model with shunt resistance. b) Effect of shunt resistance on solar cell performance. c) Complete solar cell circuit model with series & shunt resistances.

Chapter 3: Methodology

3.1 Materials

Titanium(IV) oxide (anatase nano-powder), Acetylacetone, Acetonitrile, N719 Dye (Di-tetrabutylammonium cis-bis(isothiocyanato)bis(2,2′-bipyridyl-4,4′-dicarboxylato)ruthenium(II)), Lithium Iodide, Iodine, 4-tert-Butylpyridine, Polyaniline (emeraldine salt), Glutaraldehyde solution (50%) and Polyvinyl alcohol (Hydrolyzed) were all purchased from Sigma-Aldrich Canada. All materials were used without any further purification.

3.2 Synthesis of Polyacrylamide (PAAm) Solar Cell

The cell structure was created by placing a layer of low salinity (LS) gel on a surface and curing it under UV light. Then, a layer of high salinity (HS) gel was added on top and also cured under UV light. After curing, the gels were brought together by applying light pressure. The LS gel was made of a low concentration of sodium chloride (NaCl), 2-hydroxy-4'-(2-hydroxyethoxy)-2-methylpropiophenone (also known as photo-initiator), and 37.5:1 acrylamide/N,N′-methylenebisacrylamide. The HS gel was made of a high concentration of NaCl, photo-initiator, and 37.5:1 acrylamide/N,N′-methylenebisacrylamide. The UV lamp used had a specific wavelength, distance, and time for curing the gels.

3.3 Fabrication of DSSC

i. Photoanode

FTO glass sheets were first cleaned by a detergent and deionized water followed by rinsing them with ethanol and finally dried under air. Commercial TiO_2 (anatase, surface area 45-55 m^2/g) consists of aggregated particles. To separate these particles, a porcelain mortar was used to grind 3 grams of the powder with a small amount of water

(1 mL) containing acetylacetone (0.1 mL) to prevent re-grouping. Once the powder was dispersed, the paste became more viscous, the paste was then diluted with water (4 mL) under continued grinding and a detergent (0.05 mL) was added to make it spread easily on the substrate.

To control the thickness and provide non-coated areas for electrical contact, the FTO glass was covered on two parallel edges with adhesive tape. The colloid was applied to one of the free edges and distributed with a glass rod sliding over the tape-covered edges. After air-drying, the electrode was fired for 60-80 minutes at 400 °C in air.

N719 Ruthenium complex dye was applied to the working electrode by soaking it for 24 hours in a 0.3 mM solution in dry ethanol. This was done after the high-temperature annealing to avoid rehydration of the surface or capillary condensation of water vapour in the nanopores of the film as water in the pores decreases the injection efficiency of the dye. The hot electrode (100 °C) was dipped into the dye solution and withdrawn after completion of the adsorption. It was then stored in dry ethanol or immediately wetted with a redox electrolyte solution for testing.

ii. Hydrogel Electrolyte

In this study, PVA-hydrogel was prepared through a systematic procedure involving the careful addition of varying weight percentages of polyvinyl alcohol (PVA) powder to 10 mL of 1M Sulphuric Acid. Sulfuric acid increases binding sites for hydrogel formation, leading to fast self-healing and high toughness. Additionally, it enhances conductivity through free ions. This solution was then subjected to continuous stirring for 3 hours at 90 degrees Celsius and 90 revolutions per minute (rpm) using a magnetic stirrer. The elevated temperature facilitated the dissolution of PVA and promoted the formation of a homogeneous solution.

To introduce the conductive and redox-active component, varying quantities of emeraldine salt-doped polyaniline (PANI) were incorporated into the PVA-Sulphuric Acid solution. The PANI addition was carefully metered to ensure precise control of the

composite's properties. This mixture was stirred under the same conditions as mentioned earlier for an additional 2 hours to achieve a uniform dispersion of PANI within the PVA matrix.

Subsequently, the PVA-PANI solution was allowed to cool to room temperature. Volumes of PVA-PANI solution ranging from 3 mL to 5 mL were then transferred into separate beakers, each corresponding to a particular experiment or formulation. The next step involved the introduction of varying quantities of the crosslinking agent, 25% Glutaraldehyde Solution, into the respective beakers. The purpose of this step was to initiate the crosslinking process, which is critical for the formation of the hydrogel network.

Upon the addition of Glutaraldehyde, thorough mixing ensued to ensure proper distribution within the PVA-PANI matrix. Subsequently, the crosslinked solution was transferred into petri dish, and the samples were left undisturbed overnight. This overnight period was necessary for the completion of the crosslinking reaction and the formation of the PVA-PANI hydrogel. The size and thickness of the hydrogel depend on the size of petri dish and the amount of PVA-PANI solution poured into the petri dish.

The resulting hydrogels were characterized in terms of their physical properties, such as appearance, mechanical strength, and swelling behaviour. The methodology presented here was instrumental in achieving a range of PVA-hydrogels with varying properties, allowing for an in-depth exploration of their suitability for specific applications.

The gel electrolyte was prepared by dipping small samples of dried PVA-PANI hydrogel in liquid electrolyte for about 12 hrs so that the gels reach equilibrium absorption. The liquid electrolyte consists of 0.1M lithium iodide (LiI), 0.6M I_2, 0.5M 4-tert-butylpyridine (TBP), 0.05M 1-methyl-3-propylimidazolium iodide (MPI) in a mixed solvent of N-methyl 2-pyrrolidone (NMP) and acetonitrile 2:8 ratio. The introduction of 4-tert-butylpyridine (TBP) has a profoundly positive impact on the fill factor (FF) and open-circuit voltage (Voc) of the device, signifying an enhancement in its overall efficiency. Importantly, this improvement is achieved without compromising the short-circuit photocurrent (Isc). The

increase in efficiency is a result of the dark current suppression at the junction of the semiconductor and electrolyte. The dark current occurs due to the reduction of triiodide by conduction band electrons, which still takes place despite the monolayer of N719 dye covering the TiO_2 surface. The triiodide, being relatively small in size, has the ability to cross the dye layer or access the nanometer-sized pores where the N719 dye cannot penetrate and the TiO_2 surface is bare and exposed to redox electrolyte. The TBP has the effect of slowing down the rate of triiodide reduction.

iii. Assembling DSSC

The DSSC was constructed by evenly placing the PVA-PANI gel electrolyte between the photoanodes with adsorbed dye and the counter electrode coated with pencil graphite. The devices were left for 10 minutes before taking photovoltaic measurements to allow the electrolyte to penetrate the dye-adsorbed layer.

3.4 Measurements

i. Photovoltaic Measurements

The characteristics of the photocurrent voltage curves for the DSSCs based on gel electrolytes were measured using a 100 mW cm-2 xenon arc lamp in an ambient atmosphere. The performance of the devices was evaluated by calculating the fill factor (FF) and power conversion efficiency (Ƞ) using Equations 3 and 4, respectively.

ii. Swelling Measurements of Hydrogel

Swelling is measured by the swelling ratio, which is the weight swelling ratio of the swollen gel to the dry gel. The hydrogels were soaked in for 3h.

$$Swelling\ Ratio = \frac{W_s}{W_d} \quad (7)$$

Where W_s: weight of swollen hydrogel and W_d: weight of dried hydrogel.

iii. Mechanical Measurement of Hydrogel

The mechanical stretchability of the hydrogel was observed by measuring the bending radius for the hydrogel using an vernier caliper.

Chapter 4: Results & Discussion

4.1 Effect of Preparation Method on PVA-Hydrogel

Poly(vinyl alcohol) (PVA) is a synthetic polymer that is both water-soluble and biocompatible. It contains a large number of hydroxyl functional groups, which can be cross-linked to form hydrogels. Strengthening and toughening of PVA is typically achieved through physical or chemical cross-linking. Physical cross-linking is based on intermolecular interactions, such as hydrophobic interactions, ionic/electrostatic interactions, and hydrogen bonding. This process is commonly carried out using freeze-thaw cycles, annealing, or other methods. Chemical cross-linking involves energy radiation, radical polymerization, chemical reactions between functional groups, enzyme crosslinking, and other techniques.

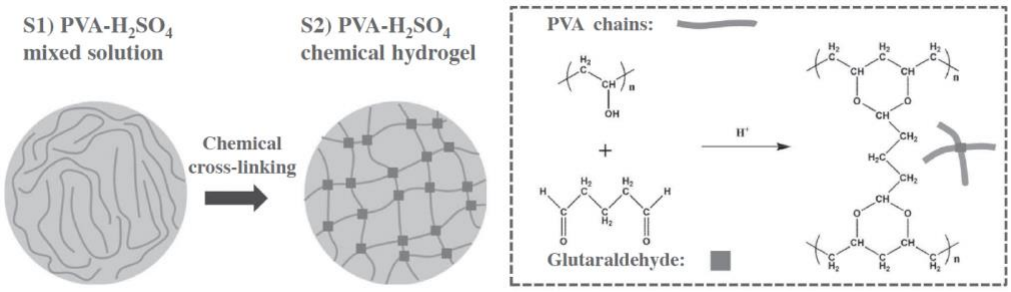


Figure 18 [35] Wang, Kai, et al. "Chemically crosslinked hydrogel film leads to integrated flexible supercapacitors with superior performance." Advanced materials 27.45 (2015): 7451-7457.

i. Effect of Physical Parameters

This study focuses on the preparation of chemically cross-linked PVA hydrogel using the crosslinking reaction between PVA and glutaraldehyde (GA). PVA's hydroxyl groups react with aldehyde groups to form acetal or hemiacetal with the aid of Sulphuric Acid as a catalyst as shown in Figure 18. The chemically cross-linked hydrogel was then constructed by controlling multiple physical cross-linking conditions such as reaction temperature and annealing while the crosslinking amount remained fixed. The study systematically observed the impact of different factors on the mechanical and swelling

properties of the hydrogel. To obtain PVA hydrogels with different properties, different treatments were taken in the gelation process as follows: (a) room temperature reaction (RT); (b) 90°C reaction (After 3 min of reaction at 90°C, the samples were cooled down to room temperature).

By increasing the reaction temperature, the polymerization reaction accelerates, causing the polymer to cross-link more quickly. When compared with PVA hydrogel prepared at room temperature, the PVA hydrogel obtained at 90°C showed significantly improved mechanical properties. However, the swelling of the hydrogel was reduced as it absorbed very little electrolyte compared to the hydrogel obtained at room temperature. This was due to the fact that the internal pores of PVA hydrogel prepared at 90°C were significantly reduced, resulting in a macroscopic structure showing certain shrinkage. In contrast, the hydrogel prepared at room temperature exhibited better-swelling properties but was mechanically weak. When hydrogel was prepared at a high temperature, it caused the gel to shrink locally and trap some of the water molecules. This leads to a higher water loss temperature (around 60°C) compared to hydrogel prepared at room temperature. This is because the trapped water molecules require a slightly higher temperature to be released.

Annealing significantly increases the strength and toughness of hydrogels obtained through room temperature reactions. This is due to the hydrogel molecular chains stacking closer together and the significant reduction in pore size. However, this process also reduces the swelling nature of the hydrogel. Meanwhile, the mechanical properties of PVA hydrogels obtained through a 90°C reaction deteriorate after annealing due to the destruction of local gelation.

In conclusion, it is evident that enhancing the mechanical strength of a hydrogel through various means invariably results in a reduction of its swelling capacity. The pursuit of greater mechanical integrity corresponds with the constriction of the hydrogel's ability to absorb and retain water. This trade-off highlights the interconnected nature of these two crucial properties and underscores the necessity for a delicate balance in hydrogel

engineering. In all, the integrated mechanical and swelling properties were best for hydrogel prepared at room temperature. Therefore, all subsequent discussions are based on samples prepared using this method.



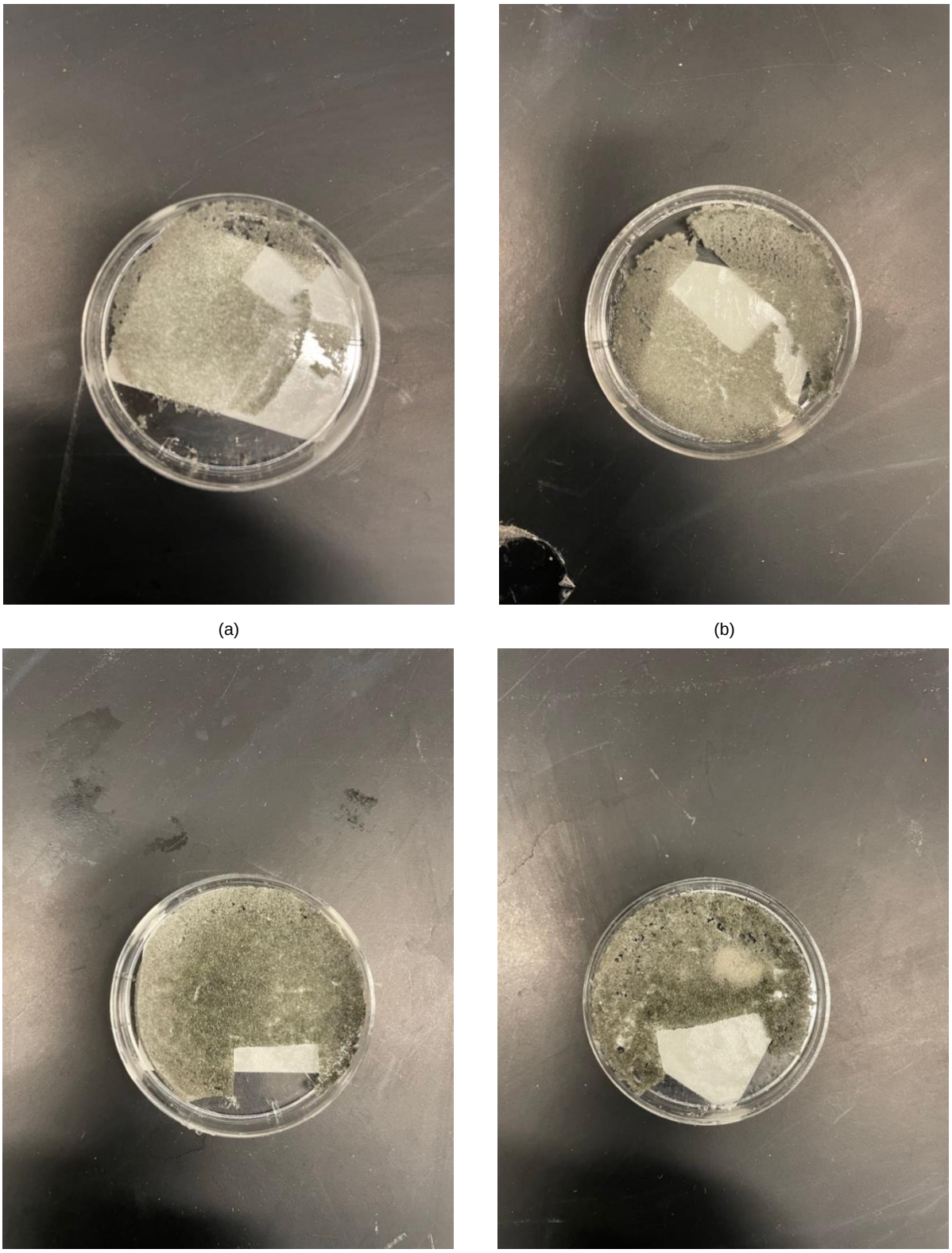
(a) (b)

Figure 19: a) Hydrogel obtained at 90°C reaction temperature. b) Hydrogel annealed after reaction at room temperature.

ii. Effect of PVA Concentrations

Five hydrogels with different concentrations of polyvinyl alcohol (PVA) (3.5 wt%, 5 wt%, 7.5 wt%, 10 wt%, and 12.5 wt%) were used to observe the effects of PVA concentration on the mechanical and swelling properties of PVA hydrogel.

The swelling nature of hydrogels with different concentrations resulted in varying pore arrangements. If the PVA content is less than 5 wt%, the resulting PVA-hydrogel film has poor mechanical strength and cannot form a free-standing film. As the mass fraction of PVA increases, the pore size also increases. At 5% mass fraction, the hydrogel has



(a) (b)

(c) (d)

Figure 20: a) 5 wt% PVA-PANI Hydrogel. b) 7.5 wt% PVA-PANI Hydrogel. c) 10 wt% PVA-PANI Hydrogel. d) 12.5 wt% PVA-PANI Hydrogel.

sparse pores, while at 10% mass fraction, it has a dense structure and moderate pore size, thus having the best mechanical properties. However, further increase in mass fraction leads to a significant increase in pore size, resulting in loosely arranged pores and fracture cracks that are easy to start in the weak network, ultimately leading to tensile fracture of the gel.

The mechanical strength of the hydrogel increases first and then decreases with increasing mass fraction. Therefore, the PVA hydrogel with a concentration of 10 wt% has the highest mechanical strength and decent swelling properties (Figure 21). Figure 20 displays images of PVA-PANI hydrogel samples with varying concentrations of PVA (while maintaining 2.5 wt% PANI concentration in all samples).

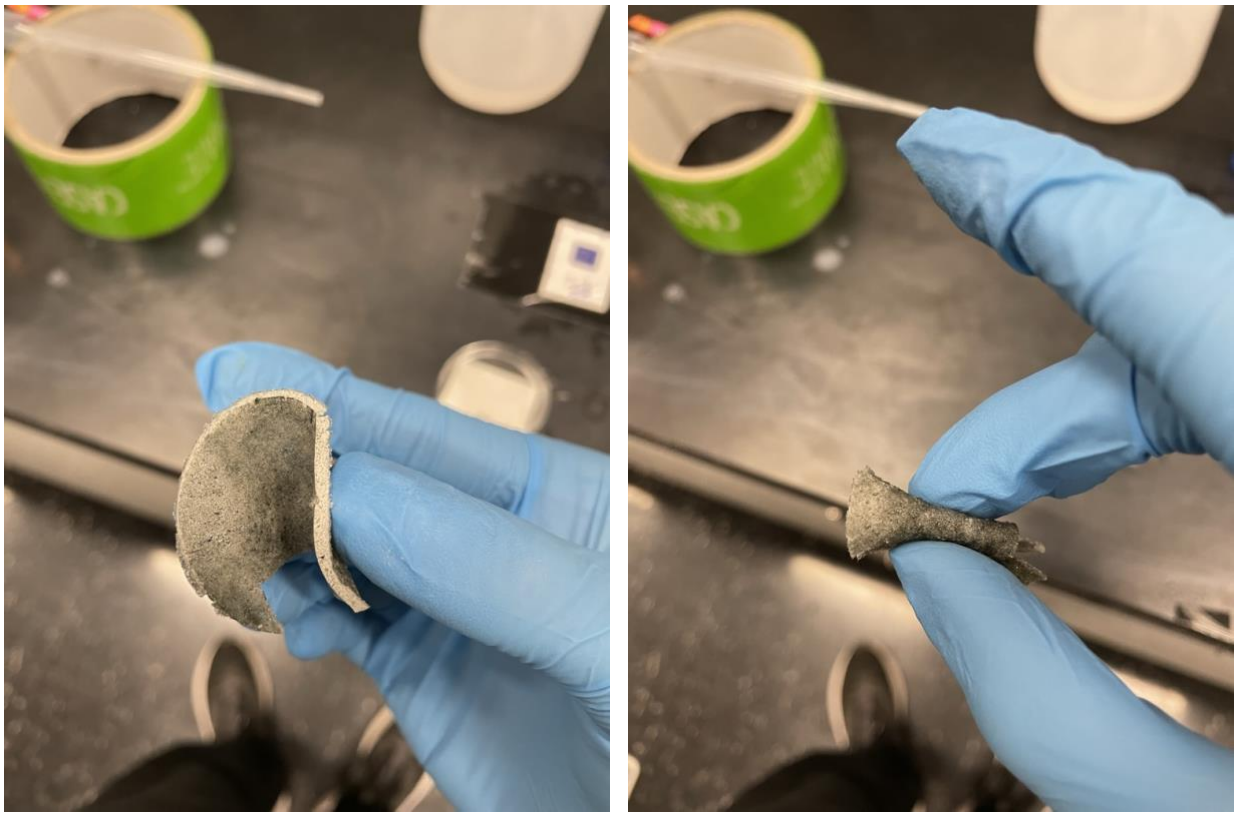


Figure 21 Stretchability of 10 wt% PVA

iii. Effect of Crosslinking

The impact of varying the crosslinker concentration on the properties of the hydrogel was investigated. The crosslinking process was carried out using a 25% glutaraldehyde (GA)

solution, with three different concentrations of crosslinker: 0.5%, 1%, and 2% of the total volume of the PVA solution.

The study revealed a clear correlation between the concentration of the crosslinker and the mechanical strength of the resulting hydrogel. As the crosslinker concentration increased from 0.5% to 2%, the hydrogel's mechanical strength improved significantly. This enhanced mechanical integrity is attributed to the increased density of crosslinks within the polymer network, which restricts the mobility of polymer chains and reduces the hydrogel's ability to swell. Consequently, the swelling behaviour of the hydrogel decreased with higher crosslinker concentrations as it can be seen in Table 2, making it less porous and more resistant to deformation. This information is crucial for tailoring hydrogels for specific applications where controlled swelling is required.

Crosslinking %	0.5%	1%	2%
Swelling Ratio	1.34	1.18	1.08

Table 2 Swelling ratio for different crosslinking ratios

A decrease in the water uptake capacity of the hydrogel was observed with higher crosslinker concentrations. This phenomenon is a direct consequence of the reduced porosity, as more crosslinks create a denser network structure that limits water absorption.

In conclusion, the investigation into the effect of crosslinking on PVA-hydrogel demonstrates that the choice of crosslinker concentration plays a pivotal role in determining the mechanical properties and swelling behaviour. For DSSC, hydrogel with 1% crosslinking was used due to its optimal swelling ratio for a mechanically stable structure.

4.2 Photovoltaic Performance of Hydrogel-Based Solar Cells

In this section, photovoltaic performance of two types of hydrogel-based solar cells were explored, namely PAAm hydrogel-based and a composite of PVA-PANI hydrogel-based

DSSC. Evaluating their photovoltaic properties, including efficiency, current-voltage characteristics, and overall performance under different conditions. The aim is to analyze and compare the outcomes of these hydrogel-based solar cells to gain insights that can contribute to the development of sustainable and efficient photovoltaic technologies. This analysis will highlight the distinctive features, challenges, and potential applications of PAAm and PVA-PANI hydrogel-based solar cells, which can shape the future of solar energy conversion devices.

i. Polyacrylamide (PAAm) Hydrogel-Based Solar Cell

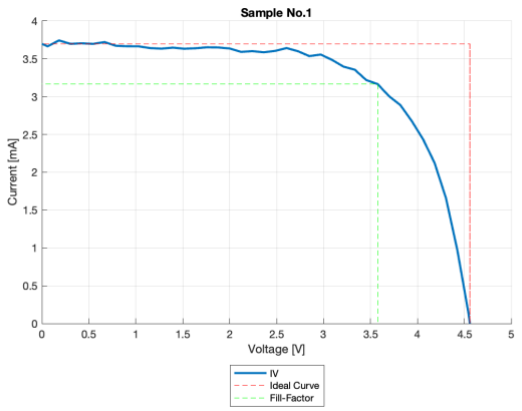
The PAAm hydrogel-based solar cell designed by the group consisted of three layers: high-salinity (HS) – low-salinity (LS) – high-salinity (HS) PAAm hydrogel. The main objective was to assess the solar cell's performance under AM1.5 conditions, where various back electrodes, such as Aluminum, Copper, and FTO (fluorine-doped tin oxide), were used. It is worth noting that the front electrode remained FTO, chosen for its transparency to allow light penetration for optimal absorption by the hydrogel. The purpose of this systematic exploration was to determine the impact of different back electrodes on the overall efficiency and functionality of the PAAm hydrogel-based solar cell.

In the investigation of various back electrodes, it was found that FTO and aluminum were the most effective for the PAAm hydrogel-based solar cell. Both configurations produced an open-circuit voltage (Voc) of around 4.5 V and a short-circuit current (Isc) of approximately 3.6 mA for a device area of 10 cm^2. Although aluminum provided slightly higher power output than FTO, the suboptimal adhesion of the hydrogel with Aluminum made FTO the preferred back electrode. This choice was strengthened by FTO's superior adhesion to the hydrogel, evident in Table 3 where the fill factor for FTO surpasses that of Aluminum. This distinction is further illustrated in the comparison of Figure 22a and 22b, where the rapid decline in the short-circuit current on the I-V curve for Aluminum as the back electrode can be attributed to its high contact resistance with the hydrogel. FTO is also chosen for its transparency, which allows for the absorption of reflected light from both sides. On the other hand, copper presented the least favorable results when used

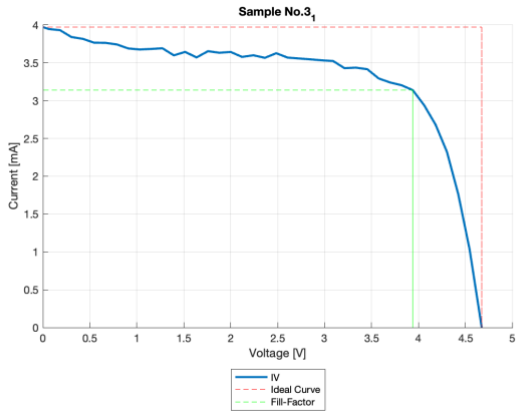
as a back electrode, with a power output of 8.05 mW and lower open-circuit voltage and short-circuit current compared to FTO and aluminum, highlighting its inferior performance in this context. Additionally, it is important to highlight that the short-circuit current (Isc) of the solar cell exhibits minimal variation with different back electrodes. This limited change in Isc can be attributed to its dependence on the concentration of salt ions in the hydrogel, which remains consistent across all devices employing various back electrodes. It is crucial to note that the Isc generated by the PAAm solar cells is notably lower than that of traditional solar cells. This disparity arises from the fact that PAAm solar cells utilize ions as charge carriers, in contrast to conventional solar cells that rely on electrons. The inherently lower mobility of ions, in comparison to electrons, results in a diminished current production by the PAAm solar cells.

Back Electrode	Device Area (cm^2)	Voc (V)	Isc (mA)	Pmax (mW)	FF (%)	Efficiency (%)
FTO	10	4.558	3.70	11.32	67.2	1.42
Aluminum	10	4.674	3.97	12.37	66.6	1.55
Copper	10	3.24	3.82	8.05	65	1.01

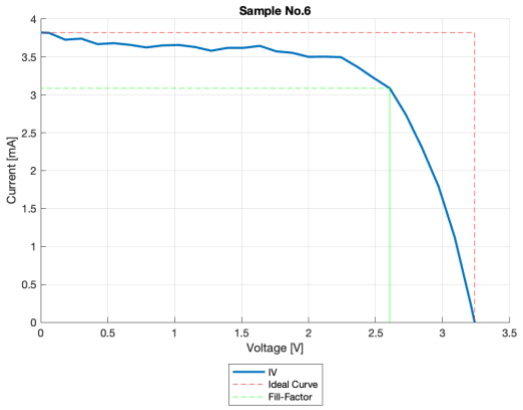
Table 3 PAAm solar cell performance with different back electrodes



(a)



(b)



(c)

Figure 22 Illuminated IV curves for different back electrodes: a) FTO b) Aluminum c) Copper

FTO was also selected as the preferred back electrode due to its superior encapsulation of the hydrogel compared to aluminum. This enhanced encapsulation ensures a more secure and robust integration of the hydrogel within the solar cell structure. The choice of FTO over aluminum reflects a consideration not only of electrical performance but also of the physical adherence and stability of the hydrogel within the solar cell, contributing to the overall efficiency and longevity of the device.

A notable aspect of the PAAm solar cell lies in its consistent output power under AM1.5 conditions, irrespective of alterations in the device area, as indicated in Table 4. Intriguingly, while adjustments to the device area did not impact the device's power output, varying the thickness of the solar cell did influence its overall performance. This observation underscores the sensitivity of the PAAm solar cell's output to changes in thickness, revealing a distinctive characteristic in its response to different structural modifications.

Back Electrode	Device Area (cm^2)	Voc (V)	Isc (mA)	Pmax (mW)	FF (%)	Efficiency (%)
FTO	2	4.219	3.77	10.11	63.5	10.11
FTO	1	4.196	3.96	11.27	67.9	11.27
FTO	0.5	4.377	3.92	11.38	66.4	22.76
FTO	0.25	4.481	3.84	11.46	66.6	45.86

Table 4 PAAm solar cell performance for different device area

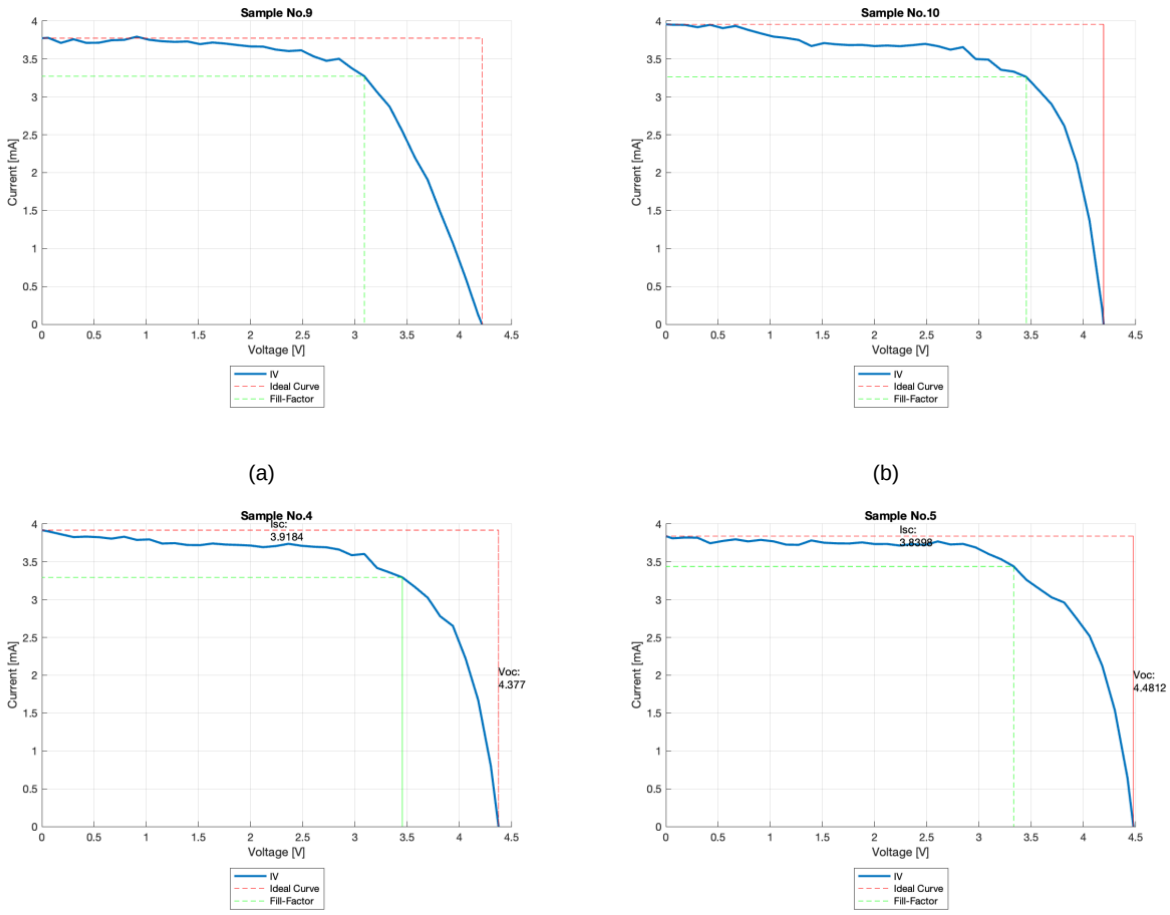


Figure 23 Illuminated IV curves for different device areas: a) $2cm^2$ b) $1cm^2$ c) $0.5cm^2$ d) $0.25cm^2$

Increasing the device thickness by 50% resulted in a decrease in power output, which is likely due to ion scattering within the layer. Collisions among ions can lead to energy dissipation, causing a loss of energy during interactions with other ions. Therefore, the ions may not have enough residual energy to effectively diffuse across layers, resulting in the observed reduction in power output. However, when the thickness of individual layers was adjusted while keeping the overall device thickness constant at 3mm, no discernible changes were observed (Table 5). This indicates that changes to individual layer thicknesses have minimal influence on the device's performance and that the overall configuration and interaction between layers are more critical in determining its behavior.

Device Area (cm^2)	Layer Thickness	Voc (V)	Isc (mA)	Pmax (mW)	FF (%)	Efficiency (%)

	Ratio (HS:LS:HS)					
1	2:1:2	4.4233	3.9576	12.39	70.75	12.39
1	1:2:3	4.271	3.8471	12.15	73.95	12.15
1	3:2:1	4.2647	3.7291	11.98	75.31	11.98
1	1:3:2	4.2746	3.8314	12.23	74.67	12.23
1	2:3:1	4.1673	3.8008	12.17	76.81	12.17

Table 5 PAAm solar cell performance for different layer thickness

The performance of PAAm hydrogel is influenced by the curing time of each layer, as longer curing times make it harder for ions to diffuse, resulting in decreased cell performance. For instance, a sample with a device area of 10 cm² and a longer curing time of 25 seconds showed a power output of 8.55 mW (Figure 24), which was nearly 3 mW lower than that of a device with a shorter curing time (Figure 22a). However, longer curing times improved the mechanical stability of the hydrogel. On the other hand, shorter curing times improved cell performance as ions moved more freely, but this came at the expense of mechanical strength. Therefore, optimizing the performance of PAAm hydrogel-based solar cells requires a delicate balance between curing time, ion diffusion, and mechanical stability.

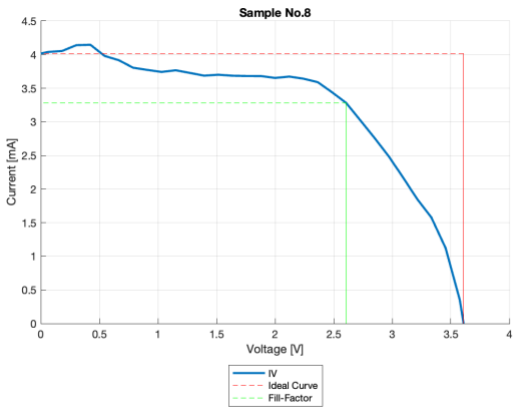


Figure 24 Illuminated IV for PAAm solar cell with increased curing time of 25s

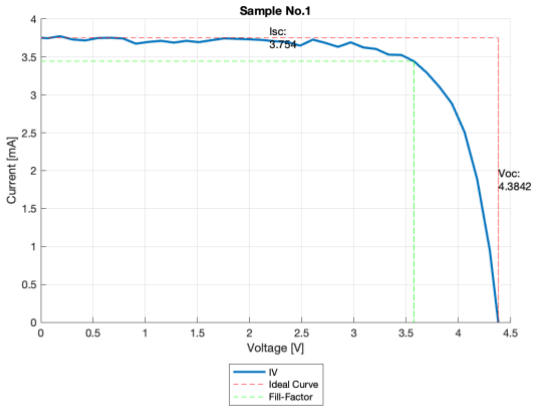
The PAAm solar cell's photovoltaic performance was evaluated under AM1.5 conditions using NaCl, KCl, and a combination of both salts. Generally, KCl has higher conductivity in water than NaCl, leading to the expectation that the solar cell's performance would be

better with KCl. However, the observed results did not align with this anticipated trend. Surprisingly, the PAAm solar cell with only NaCl had better performance compared to its KCl counterpart. This discrepancy suggests that other factors beyond conductivity are significant in determining the solar cell's efficiency. This emphasizes the intricate interplay of various elements in influencing the overall performance of the hydrogel-based solar cell.

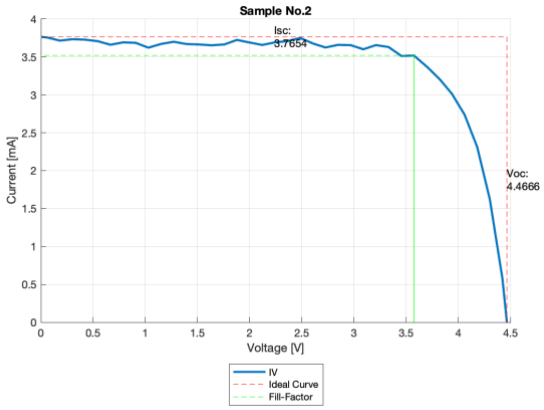
Further experiments were carried out on a modified two-layer device consisting of only high-salinity and low-salinity layers, instead of the original three-layered HS-LS-HS structure. Interestingly, the outcomes obtained from the two-layer configuration were similar to those achieved with the three-layer design, indicating that the simplified structure can have a comparable performance without compromising its effectiveness. This suggests that the design of the PAAm hydrogel-based solar cell can be streamlined while maintaining its photovoltaic efficiency. Additionally, tests were performed on 2-layered cells connected both in series and in parallel, revealing distinct electrical behaviors. As predicted, the combined voltage of cells attached in a series demonstrated an expected accumulation. Nevertheless, when connected in parallel, the current did not exhibit an additive pattern. Table 6 presents the outcomes of the performance measurements for individual cells, along with the results when these cells were connected in series. The findings provide valuable insights for optimizing and understanding the PAAm hydrogel-based solar cell system.

	Device Area (cm^2)	Voc (V)	Isc (mA)	Pmax (mW)	FF (%)	Efficiency (%)
Cell 1	1	4.3842	3.754	12.31	74.82	12.31
Cell 2	1	4.4666	3.7654	12.58	74.82	12.58
Cell 1-2 in Series	2	8.8539	3.7637	25.55	76.68	12.78

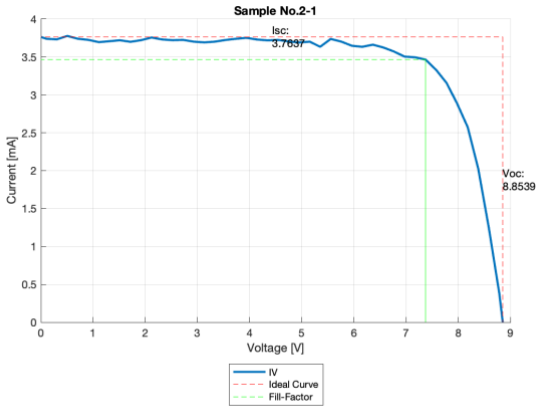
Figure 25 2-layered (HS-LS) PAAm solar cell performance



(a)



(b)



(c)



(d)

Figure 26: a) Cell 1 illuminated IV. b) Cell 2 illuminated IV. c) Illuminated IV for cell 1-2 in series. d) Picture of Cell 1 & 2 in Series

ii. PVA-PANI Hydrogel-Based DSSC

The utilization of PVA-PANI hydrogel soaked with an iodide/triiodide electrolyte as a quasi-solid-state electrolyte for Dye-Sensitized Solar Cells (DSSCs) represents a

fascinating avenue for enhancing the performance of these renewable energy devices. In this study, two different concentrations of PANI were employed within the hydrogel, specifically 2.5 wt% and 5 wt% of the PVA (shown in Figure 27), to investigate the influence of PANI content on the DSSC's electrical characteristics. The primary focus was on the short-circuit current (Isc) and the open-circuit voltage (Voc), crucial parameters defining the overall efficiency of a solar cell.



(a) (b)

Figure 27: a) 2.5 wt% PANI hydrogel. b) 5 wt% PANI hydrogel.

A key finding of this study is that the short-circuit current (Isc) of the DSSC increases significantly with the increase in PANI content in the PVA-PANI hydrogel. This can be attributed to multiple factors. Firstly, the introduction of PANI within the PVA-PANI hydrogel significantly enhances the electrical conductivity of the electrolyte, which improves charge transport. Dark IV measurements were used to assess the electrical conductivity of the PVA-PANI hydrogel with varying PANI concentrations (2.5 wt% and 5 wt%). This data can provide insights into the intrinsic electrical properties of the hydrogel

as a function of PANI content. Comparing the conductivity of the two hydrogel samples revealed that higher PANI content leads to improved electron and ion transport within the material as it can be seen in Figure 28 that hydrogel with 5 wt% PANI has better electrical conductivity than 2.5 wt%. Polyaniline is an excellent candidate for improving charge transport as it is a conducting polymer with high intrinsic conductivity. This enhanced conductivity allows for more efficient movement of electrons and ions within the hydrogel, reducing charge recombination losses. It also facilitates more efficient electron transfer from the dye-sensitized photoanode to the counter electrode, ultimately enhancing the overall current-carrying capacity of the DSSC.

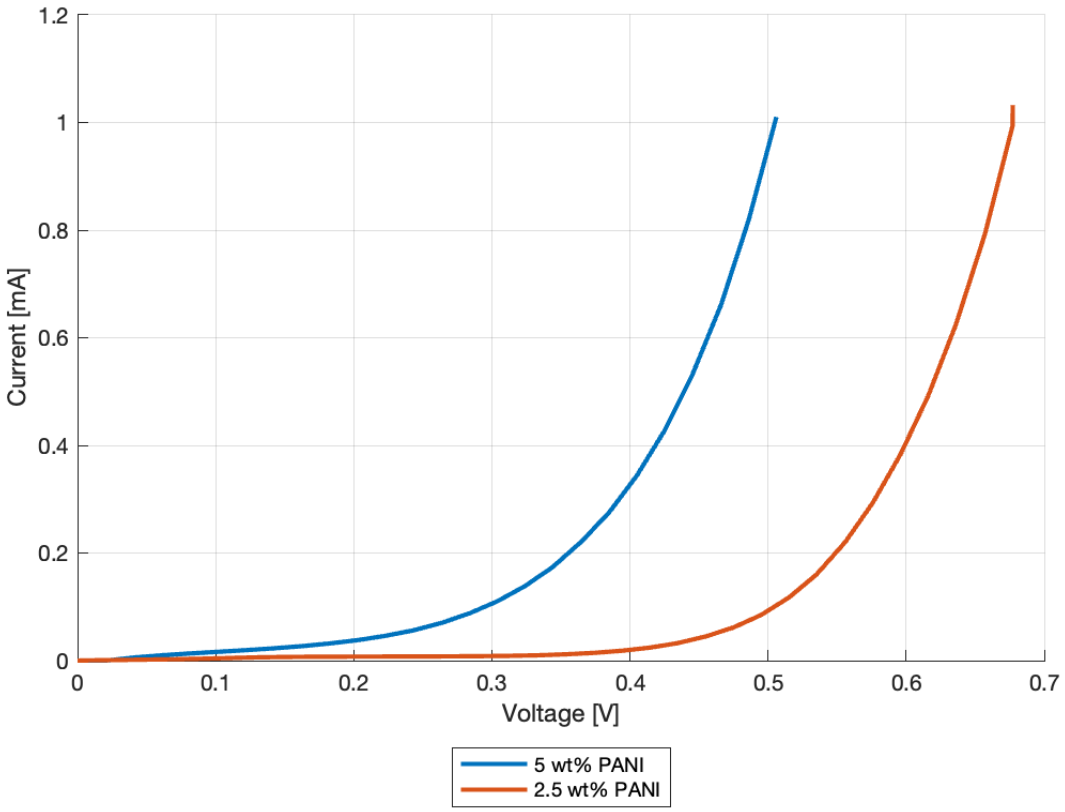


Figure 28 Dark IV of DSSC with different concentrations of PANI

The presence of PANI in the hydrogel improves electrical conductivity, which makes it easier for electrons to be injected from photoexcited dye molecules into the photoanode's conduction band. This critical step facilitates the conversion of light energy to electrical

energy in a DSSC. The reduced resistance in the hydrogel promotes rapid electron injection, leading to a more efficient charge separation process. Besides, PANI in the hydrogel can also facilitate the movement of triiodide ions (I_3^-) in the electrolyte. PANI's high ionic conductivity aids in the I_3^- ion movement, which plays a crucial role in DSSC's redox reactions. Efficient ion transport results in better charge regeneration and reduces losses due to diffusion limitations.

One of the major factors that affect the efficiency of DSSCs is charge recombination, which occurs when photogenerated electrons combine with oxidized species before reaching the external circuit. The PVA-PANI hydrogel has enhanced conductivity, which reduces the likelihood of charge recombination by allowing electrons and holes to travel quickly to the respective electrodes. This, in turn, minimizes losses in the recombination process. The use of PVA-PANI hydrogel soaked in an iodide/triiodide electrolyte can also contribute to the long-term stability of the DSSC. Hydrogels are known for their excellent liquid retention properties, ensuring that the electrolyte is consistently present within the device. This feature helps maintain the device's performance over time and is particularly beneficial in real-world applications.

	Isc	Voc
Liquid Electrolyte	0.07 mA	0.13V
2.5 wt% PANI Hydrogel	0.09 mA	0.17V
5 wt% PANI Hydrogel	0.32 mA	0.15V

Table 6 Isc & Voc for different electrolytes

Throughout the investigation, it was observed that the Voc of the DSSC remained relatively constant, irrespective of the varying concentrations of PANI in the PVA-PANI hydrogel as mentioned in Table 7. The open-circuit voltage is primarily determined by the difference in electrochemical potential between the redox couple in the electrolyte and the conduction band of the photoanode. Despite the presence of PANI in the hydrogel, this electrochemical potential difference was not significantly affected, resulting in a stable Voc. The consistency in Voc is crucial as it means that the voltage characteristics of the cell are not compromised by the presence of varying PANI concentrations.

Furthermore, PANI was also deposited on the counter electrode, dispersing it in dry ethanol first and letting it dry on the FTO to increase the short circuit current of the device. Doing this increased the efficiency of the device to 1.07% with a device area of 0.5 cm^2. Figure 29 shows the illuminated IV for the DSSC.

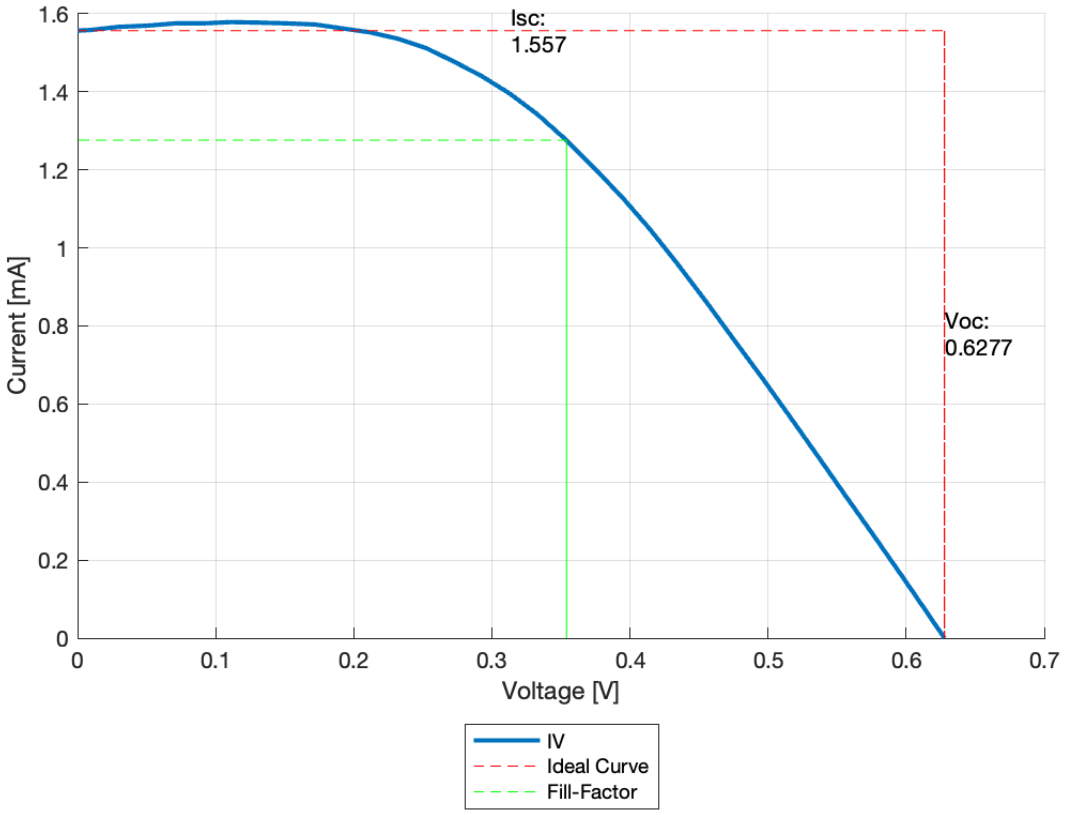


Figure 29 Illuminated IV for hydrogel based DSSC.

To evaluate the feasibility of the hydrogel-based Dye-Sensitized Solar Cell (DSSC) concept, a proof-of-concept experiment was conducted, along with a comprehensive lifetime analysis. The experiment involved placing the cell under a desk lamp to simulate practical indoor lighting conditions. The open circuit voltage and short circuit current were measured at different intervals, extending beyond the calculated half-life of the cell, which is approximately 3 hours. Next, the obtained data was used to create a graph that demonstrates the normalized values of short circuit current and open circuit voltage over

time (Figure 30). This temporal analysis offers valuable insights into the stability and performance dynamics of the hydrogel-based DSSC. These insights are crucial for understanding its potential for extended operational longevity and efficiency. The observed trends and patterns in the graph contribute essential information to the broader investigation into the applicability of hydrogel-based quasi-solid-state electrolytes in DSSCs.

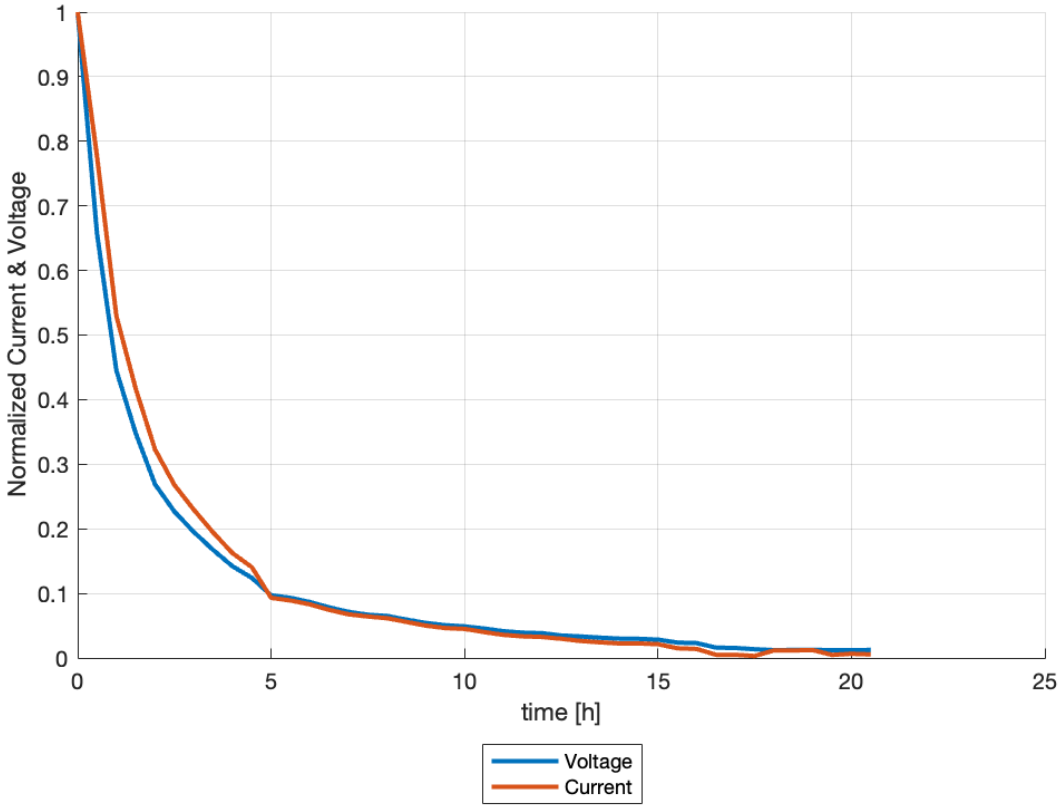


Figure 30 Proof of Concept

Chapter 5: Conclusion

The investigation of PAAm hydrogel-based solar cells has provided valuable insights into their unique characteristics and challenges. The PAAm solar cell design, which consists of three layers including high-salinity (HS) and low-salinity (LS) layers, demonstrated promising performance under AM1.5 conditions. The selection of materials, such as FTO and aluminum as back electrodes, played a significant role in achieving optimal outcomes. The study also revealed the critical impact of curing time on device performance, emphasizing the importance of finding a delicate balance between mechanical stability and power generation.

Despite its successes, the investigation also revealed some drawbacks. Specifically, the PAAm solar cell was found to be less responsive to alterations in thickness, and prolonged curing times had negative impacts on ion diffusion. To address these issues, a new approach was taken, involving a two-layered structure that emphasized HS and LS layers. This revised design yielded similar results, indicating that a simpler configuration could be just as effective.

Two main challenges were faced in designing the Polyacrylamide (PAAm) hydrogel. The first challenge was the inability to restore the potential gradient within the device after operation, which was a significant limitation. Secondly, relying solely on hydrogels as the primary light absorber restricted the device's photon absorption capabilities in the visible range. Therefore, incorporating photoactive compounds was necessary to enhance absorption. To address these challenges, the Polyvinyl Alcohol-Polyaniline (PVA-PANI) Dye-Sensitized Solar Cell (DSSC) was chosen as a strategic solution.

In the future, there is potential for enhancement through the proposed creation of a DSSC using a PVA-PANI hydrogel design. By utilizing the benefits of PVA-PANI, such as improved electrical conductivity and flexibility, the goal is to overcome the limitations seen in PAAm hydrogel-based solar cells. The envisioned DSSC design shows promise for

achieving better efficiency, durability, and adaptability, providing a path for advancing hydrogel-based solar cells. To summarize, the use of a PVA-PANI hydrogel soaked in an iodide/triiodide electrolyte has significantly improved the lifetime performance of the solar cell. The PANI component of the hydrogel has played a key role in enhancing the charge transport and reducing charge recombination. Additionally, it has also improved ion transport, leading to higher photocurrent generation and increased efficiency in converting light to electricity. These enhancements suggest that this system holds great promise for the future of renewable energy, particularly in advancing the efficiency and practicality of DSSCs.

The findings from this study are particularly significant as they demonstrate that increasing the PANI concentration within the PVA-PANI hydrogel serves to improve the Isc without affecting the Voc. This observation suggests that PVA-PANI hydrogel with 5 wt% PANI content can be effectively utilized as a quasi-solid-state electrolyte for DSSCs, offering the advantage of enhanced photocurrent generation without altering the voltage characteristics of the cell. This result implies that PVA-PANI hydrogel electrolytes have great potential for improving the performance of DSSCs, thus contributing to the development of more efficient and sustainable solar energy conversion technologies.

Moreover, it's important to recognize that the findings of this study present exciting opportunities for further exploration. Future research may delve deeper into the underlying mechanisms responsible for the improvement in photocurrent with higher PANI concentrations, allowing for more targeted optimization of DSSCs and expanding their application in the field of renewable energy. The PVA-PANI hydrogel electrolyte system holds the promise of contributing to the advancement of environmentally friendly energy solutions. This research contributes to the development of sustainable energy solutions, leading the way for innovations that bridge the gap between efficiency and practicality in hydrogel-based photovoltaic devices.

5.1 Future Prospects

The research presented in this thesis provides a foundation for exciting future prospects in the field of hydrogel-based Dye-Sensitized Solar Cells (DSSCs). By utilizing hydrogel materials, there are several promising directions for further exploration and innovation. This project aims to investigate a novel approach to DSSC technology by using hydrogel materials for both the working electrode and the counter electrode. This approach intends to improve the overall performance and stability of these solar cells.

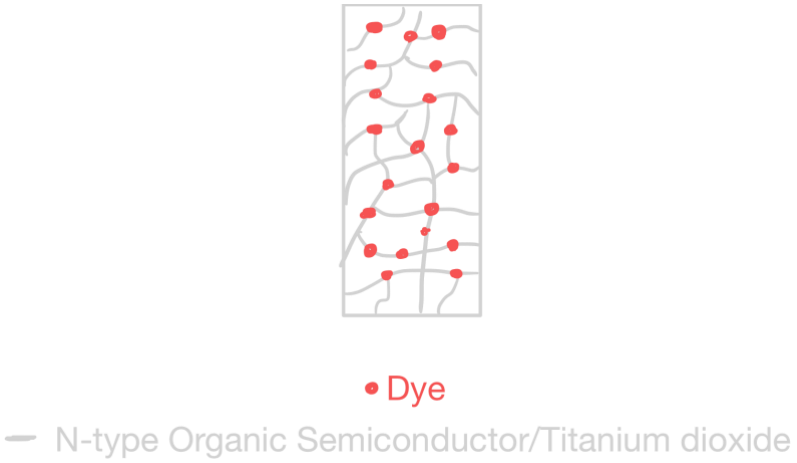


Figure 31 Proposed Working Electrode

Semiconductor layers are typically attached to various substrates through physical adsorption. However, they remain as two-dimensional (2D) materials on the substrate, which results in the different efficiency of light energy inside and outside the material. This leads to a decrease in overall photocurrent efficiency since only the surface of the material can effectively utilize the light energy. To address this issue, we require a three-dimensional (3D) material with excellent light transmittance. One way to achieve this is by using hydrogel as the substrate for the working electrode. By coating the hydrogel with either an N-type organic semiconductor or titanium dioxide (TiO2) as the electron acceptor material and attaching dye molecules to the semiconductor for efficient light absorption and charge separation (Figure 14), the dye inside the hydrogel can receive light uniformly and make full use of the light energy to improve the photocurrent. Hydrogels possess a three-dimensional porous structure and a suitable nanopore size distribution, which provide a large number of reaction sites for the dye and the electrolyte.

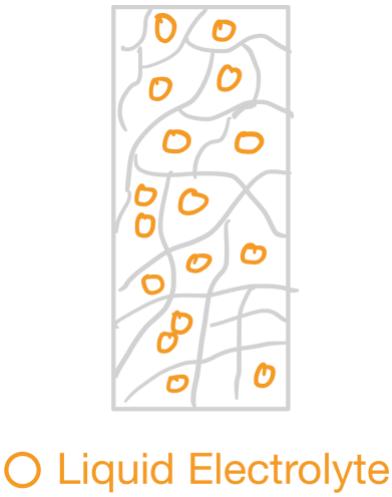


Figure 32 Proposed hydrogel-based electrolyte

Introducing a hydrogel layer swelled with a liquid electrolyte acts as a container for the liquid electrolyte. Doing this ensures that the liquid doesn't leak and provides stability to the device ensuring efficient ionic conduction and electron transfer. Furthermore, this hydrogel can be made pH-sensitive with certain anionic or cationic groups to reduce the exciton recombination (Figure 15).



Figure 33 Proposed Counter Electrode

To enhance the electrocatalytic properties of the counter electrode through PANI coating a PANI-hydrogel based counter electrode through in-situ polymerization will be used as the counter electrode (Figure 16). Developing a counter electrode using a hydrogel substrate and coating the hydrogel with polyaniline (PANI) to facilitate efficient charge

transfer and reduction of the electrolyte. 3D structure of the hydrogel will provide many reduction sites for the ions thus decreasing the recombination of the excitons.

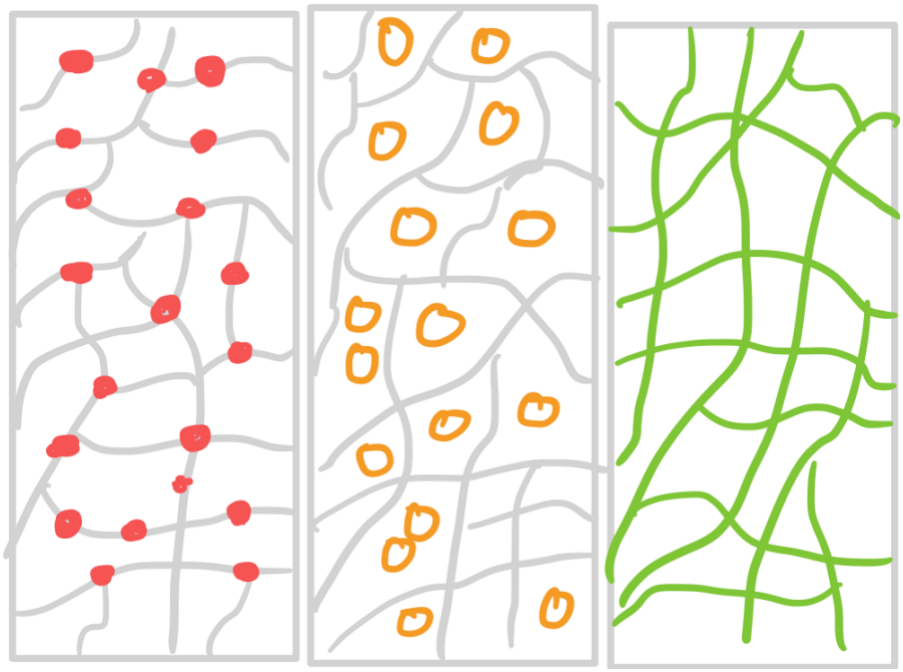


Figure 34 Proposed DSSC

References

[1] Tributsch, Helmut. "Reaction of excited chlorophyll molecules at electrodes and in photosynthesis." *Photochemistry and Photobiology* 16.4 (1972): 261-269.

[2] O'regan, Brian, and Michael Grätzel. "A low-cost, high-efficiency solar cell based on dye-sensitized colloidal TiO2 films." *nature* 353.6346 (1991): 737-740.

[3] Schroeder, Thomas BH, et al. "An electric-eel-inspired soft power source from stacked hydrogels." *Nature* 552.7684 (2017): 214-218.

[4] Kang, Seong Min, et al. "Moth-eye TiO2 layer for improving light harvesting efficiency in perovskite solar cells." *Small* 12.18 (2016): 2443-2449.

[5] Kirschner, Chelsea M., and Kristi S. Anseth. "Hydrogels in healthcare: from static to dynamic material microenvironments." Acta materialia 61.3 (2013): 931-944.

[6] Han, Jingquan, et al. "A self-healable and highly flexible supercapacitor integrated by dynamically cross-linked electro-conductive hydrogels based on nanocellulose-templated carbon nanotubes embedded in a viscoelastic polymer network." Carbon 149 (2019): 1-18.

[7] Park, Junggeon, et al. "Micropatterned conductive hydrogels as multifunctional muscle-mimicking biomaterials: Graphene-incorporated hydrogels directly patterned with femtosecond laser ablation." *Acta biomaterialia* 97 (2019): 141-153.

[8] Ganguly, Sayan, et al. "Mechanically robust dual responsive water dispersible-graphene based conductive elastomeric hydrogel for tunable pulsatile drug release." *Ultrasonics sonochemistry* 42 (2018): 212-227.

[9] Guarino, Vincenzo, et al. "Conductive PANi/PEGDA macroporous hydrogels for nerve regeneration." *Advanced healthcare materials* 2.1 (2013): 218-227.

[10] Ren, Kai, et al. "Self-healing conductive hydrogels based on alginate, gelatin and polypyrrole serve as a repairable circuit and a mechanical sensor." *Journal of Materials Chemistry B*7.37 (2019): 5704-5712.

[11] Pattavarakorn, Datchanee, et al. "Electroactive performances of conductive polythiophene/hydrogel hybrid artificial muscle." *Energy Procedia* 34 (2013): 673-681.

[12] Reddy, Narendra, et al. "Effect of glutaraldehyde crosslinking conditions on the strength and water stability of wheat gluten fibers." *Macromolecular materials and engineering* 293.7 (2008): 614-620.

[13] Magami, Saminu Musa, et al. "The physical–chemical behaviour of amino cross-linkers and the effect of their chemistry on selected epoxy can coatings' hydrolysis to melamine and to formaldehyde into aqueous food simulants." *Progress in Organic Coatings* 78 (2015): 325-333.

[14] Yokoyama, F., et al. "Morphology and structure of highly elastic poly (vinyl alcohol) hydrogel prepared by repeated freezing-and-melting." *Colloid and Polymer Science* 264 (1986): 595-601.

[15] Cascone, MARIA GRAZIA, et al. "Effect of chitosan and dextran on the properties of poly (vinyl alcohol) hydrogels." *Journal of Materials science: Materials in medicine* 10 (1999): 431-435.

[16] Buenger, Daniel, Fuat Topuz, and Juergen Groll. "Hydrogels in sensing applications." *Progress in Polymer Science* 37.12 (2012): 1678-1719.

[17] Buenger, Daniel, Fuat Topuz, and Juergen Groll. "Hydrogels in sensing applications." *Progress in Polymer Science* 37.12 (2012): 1678-1719.

[18] Qi, Xiaoliang, et al. "Investigation of Salecan/poly (vinyl alcohol) hydrogels prepared by freeze/thaw method." *Carbohydrate polymers* 118 (2015): 60-69.

[19] Chen, Qiao, et al. "Effect of different gel electrolytes on graphene-based solid-state supercapacitors." *RSC advances* 4.68 (2014): 36253-36256.

[20] Wang, Zifeng, et al. "Hydrogel electrolytes for flexible aqueous energy storage devices." *Advanced Functional Materials* 28.48 (2018): 1804560.

[21] Wang, Kai, et al. "Chemically crosslinked hydrogel film leads to integrated flexible supercapacitors with superior performance." *Advanced materials* 27.45 (2015): 7451-7457.

[22] Lei, Zhouyue, et al. "A bioinspired mineral hydrogel as a self-healable, mechanically adaptable ionic skin for highly sensitive pressure sensing." *Advanced Materials* 29.22 (2017): 1700321.

[23] Keplinger, Christoph, et al. "Stretchable, transparent, ionic conductors." *Science* 341.6149 (2013): 984-987.

[24] Yang, Can Hui, et al. "Electroluminescence of giant stretchability." *Advanced Materials* 28.22 (2016): 4480-4484.

[25] Larson, Christina, et al. "Highly stretchable electroluminescent skin for optical signaling and tactile sensing." *science* 351.6277 (2016): 1071-1074.

[26] Sharma, Khushboo, Vinay Sharma, and S. S. Sharma. "Dye-sensitized solar cells: fundamentals and current status." *Nanoscale research letters* 13 (2018): 1-46.

[27] Shalini, S., et al. "Status and outlook of sensitizers/dyes used in dye sensitized solar cells (DSSC): a review." International journal of energy research 40.10 (2016): 1303-1320.

[28] Lin, Lu Yin, and Kuo Chuan Ho. "Dye-sensitized solar cells." *Encyclopedia of Modern Optics*. Elsevier, 2018. 270-281.

[29] Huang, Huabo, et al. "Reinforced polyaniline/polyvinyl alcohol conducting hydrogel from a freezing–thawing method as self-supported electrode for supercapacitors." *Journal of materials science* 51 (2016): 8728-8736.

[30] Li, Wanwan, et al. "Strong and robust polyaniline-based supramolecular hydrogels for flexible supercapacitors." Angewandte Chemie 128.32 (2016): 9342-9347.

[31] Nazeeruddin, M. Khaja, et al. "Conversion of light to electricity by cis-X2bis (2, 2'-bipyridyl-4, 4'-dicarboxylate) ruthenium (II) charge-transfer sensitizers (X= Cl-, Br-, I-, CN-, and SCN-) on nanocrystalline titanium dioxide electrodes." Journal of the American Chemical Society 115.14 (1993): 6382-6390.

[32] Khannam, Momina, et al. "A graphene oxide incorporated TiO2 photoanode for high efficiency quasi solid state dye sensitized solar cells based on a poly-vinyl alcohol gel electrolyte." RSC advances 6.60 (2016): 55406-55414.

[33] Nazeeruddin, Md K., Etienne Baranoff, and Michael Grätzel. "Dye-sensitized solar cells: A brief overview." Solar energy 85.6 (2011): 1172-1178.

[34] Nazeeruddin, Mohammad K., et al. "Combined experimental and DFT-TDDFT computational study of photoelectrochemical cell ruthenium sensitizers." *Journal of the American Chemical Society* 127.48 (2005): 16835-16847.

[35] Kay, Andreas, and Michael Grätzel. "Low cost photovoltaic modules based on dye sensitized nanocrystalline titanium dioxide and carbon powder." *Solar Energy Materials and Solar Cells* 44.1 (1996): 99-117.

[36] Nath, Bikash Chandra, et al. "High performance polyvinyl alcohol/multi walled carbon nanotube/polyaniline hydrogel (PVA/MWCNT/PAni) based dye sensitized solar cells." Electrochimica Acta 146 (2014): 106-111.

[37] Karakuş, Mücella Özbay, et al. "A roadmap for hydrogel-based quasi-solid electrolyte preparation for use in dye-sensitized solar cell." Electrochimica Acta 427 (2022): 140841.

[38] Li, Qinghua, et al. "Application of microporous polyaniline counter electrode for dye-sensitized solar cells." Electrochemistry Communications 10.9 (2008): 1299-1302.

[39] Zhang, D. W., et al. "Graphene-based counter electrode for dye-sensitized solar cells." Carbon 49.15 (2011): 5382-5388.

[40] Tao, Yulun, et al. "TiO2/PANI/Graphene–PVA hydrogel for recyclable and highly efficient photo-electrocatalysts." Industrial & Engineering Chemistry Research 60.28 (2021): 10033-10043.